Short Article

Cell Stem Cell

Th17 Lymphocytes Induce Neuronal Cell Death in a Human iPSC-Based Model of Parkinson's Disease

Graphical Abstract

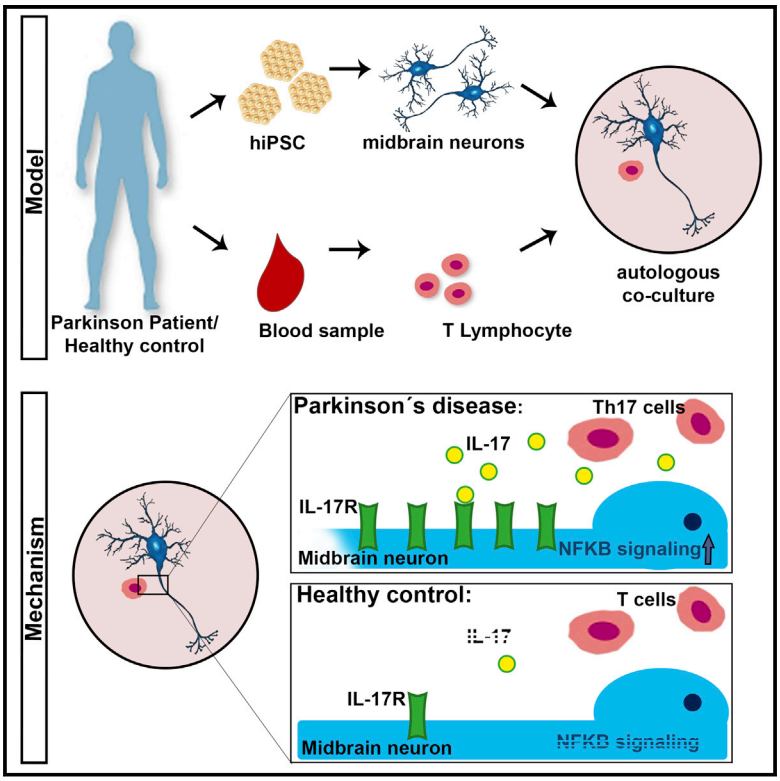

Highlights

- Increased numbers of T cells are detected in PD postmortem midbrains
- Increased frequencies of IL-17-producing T cells are found in PD patients' blood
- T cells induce neuronal death in PD revealed by human autologous iPSC-based model
- Neuronal cell death is mediated by IL-17–IL-17R signaling and activation of NFκB

Authors

Annika Sommer, Franz Maxreiter, Florian Krach, ..., Jürgen Winkler, Iryna Prots, Beate Winner

Correspondence

iryna.prots@uk-erlangen.de

In Brief

The role of lymphocytes in PD pathology was studied. Increased T cell numbers and frequencies of Th17 cells were detected in PD brains and in PD patients' blood, respectively. T lymphocytes induced cell death in PD iPSC-derived neurons mediated by IL-17, indicating an important role for T cells in PD.

Sommer et al., 2018, Cell Stem Cell *23*, 123–131
July 5, 2018
https://doi.org/10.1016/j.stem.2018.06.015

CellPress

Cell Stem Cell
Short Article

Th17 Lymphocytes Induce Neuronal Cell Death in a Human iPSC-Based Model of Parkinson's Disease

Annika Sommer,[1,2,9] Franz Maxreiter,[3] Florian Krach,[1,4] Tanja Fadler,[2] Janina Grosch,[3] Michele Maroni,[1,5] Daniela Graef,[1,2] Esther Eberhardt,[1,5] Markus J. Riemenschneider,[6] Gene W. Yeo,[4] Zacharias Kohl,[3] Wei Xiang,[7] Fred H. Gage,[8] Jürgen Winkler,[3] Iryna Prots,[1,2,10,11,*] and Beate Winner[1,2,10]

[1]Department of Stem Cell Biology, Friedrich-Alexander-Universität (FAU) Erlangen-Nürnberg, 91054 Erlangen, Germany
[2]IZKF Junior Research Group 3 and BMBF Research Group Neuroscience, Interdisciplinary Center for Clinical Research, Friedrich-Alexander-Universität (FAU) Erlangen-Nürnberg, 91054 Erlangen, Germany
[3]Department of Molecular Neurology, Universitätsklinikum Erlangen, Friedrich-Alexander-Universität (FAU) Erlangen-Nürnberg, 91054 Erlangen, Germany
[4]Department of Cellular and Molecular Medicine, University of California, San Diego, La Jolla, CA 92037, USA
[5]Department of Anesthesiology, Friedrich-Alexander-Universität (FAU) Erlangen-Nürnberg, 91054 Erlangen, Germany
[6]Department of Neuropathology, Regensburg University Hospital, 93053 Regensburg, Germany
[7]Institute of Biochemistry (Emil-Fischer-Center), Friedrich-Alexander-Universität (FAU) Erlangen-Nürnberg, 91054 Erlangen, Germany
[8]Laboratory of Genetics, Salk Institute for Biological Studies, La Jolla, CA 92037, USA
[9]Present address: Evotec AG, Manfred Eigen Campus, 22419 Hamburg, Germany
[10]These authors contributed equally
[11]Lead Contact
*Correspondence: iryna.prots@uk-erlangen.de
https://doi.org/10.1016/j.stem.2018.06.015

SUMMARY

Parkinson's disease (PD) is a neurodegenerative disorder characterized by the progressive degeneration of midbrain neurons (MBNs). Recent evidence suggests contribution of the adaptive immune system in PD. Here, we show a role for human T lymphocytes as cell death inducers of induced pluripotent stem cell (iPSC)-derived MBNs in sporadic PD. Higher Th17 frequencies were found in the blood of PD patients and increased numbers of T lymphocytes were detected in postmortem PD brain tissues. We modeled this finding using autologous co-cultures of activated T lymphocytes and iPSC-derived MBNs of sporadic PD patients and controls. After co-culture with T lymphocytes or the addition of IL-17, PD iPSC-derived MBNs underwent increased neuronal death driven by upregulation of IL-17 receptor (IL-17R) and NFκB activation. Blockage of IL-17 or IL-17R, or the addition of the FDA-approved anti-IL-17 antibody, secukinumab, rescued the neuronal death. Our findings indicate a critical role for IL-17-producing T lymphocytes in sporadic PD.

INTRODUCTION

Aberrant regulation of T lymphocyte activation during the adaptive immune response to infections or to self-antigens may trigger a strong immune reaction and result in uncontrolled inflammation. This mechanism is evident in several chronic inflammatory autoimmune disorders, including those of the central nervous system (CNS) like multiple sclerosis (MS), Sydenham's chorea, or Pediatric Autoimmune Neuropsychiatric Disorders Associated with *Streptococcus* infections, which are characterized by pronounced neurodegeneration due to a chronic T lymphocyte-driven inflammation (Cutforth et al., 2016; Dendrou et al., 2015).

Parkinson's disease (PD) is a chronic neurodegenerative disorder characterized by the progressive degeneration of midbrain neurons (MBNs) in the substantia nigra (SN) pars compacta. A crucial role of inflammation for neurodegeneration in PD is well established and mainly attributed to innate immune cells of the CNS (Hirsch et al., 2012; Ransohoff, 2016). The potential contribution of the adaptive immune system in human PD pathogenesis remains elusive. While CD4+ and CD8+ T lymphocytes have been shown to be present in postmortem brain tissues of PD patients (Brochard et al., 2009) and alterations of T cell subsets in the blood of PD patients have been reported (Baba et al., 2005; Bas et al., 2001; Stevens et al., 2012), it is still unclear whether and how they contribute to neurodegeneration. Interestingly, a recent study demonstrated activation of T lymphocytes from PD patients by α-synuclein, suggesting a possible role of autoimmune inflammation in PD pathogenesis (Sulzer et al., 2017).

Animal models have provided several indications of T lymphocyte involvement in PD pathology (Brochard et al., 2009; Reynolds et al., 2010). However, it remains challenging to prove that the implicated neurodegenerative mechanisms are also evident in human neurons. Thus, new investigative models are required to determine the impact of T lymphocytes on neurons in human PD pathogenesis. The discovery of human induced pluripotent stem cells (hiPSCs) opens up the unique possibility of modeling disease in a human cellular system (Lee and Studer, 2010; Takahashi et al., 2007). Indeed, hiPSC studies of monogenic PD have already reproduced PD-associated phenotypes (Borgs et al., 2016; Byers et al., 2011; Nguyen et al., 2011; Ryan et al., 2013; Shaltouki et al., 2015). The derivation of hiPSC

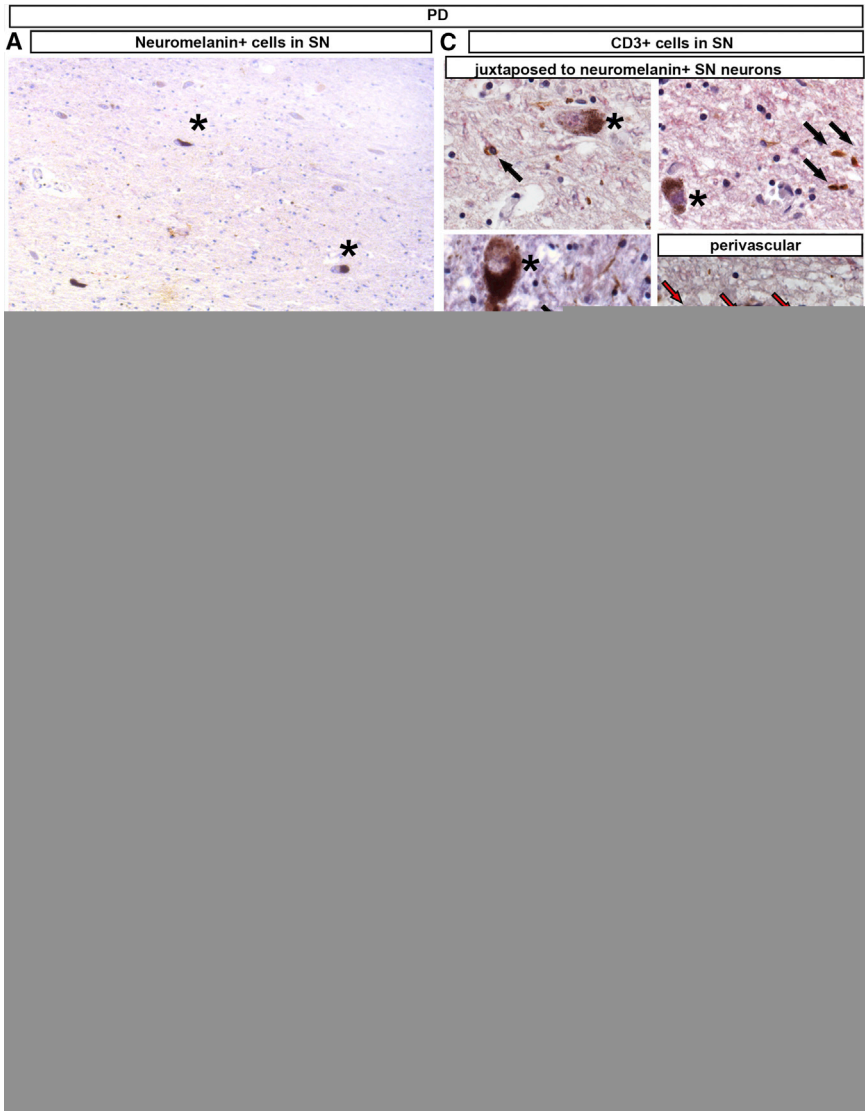

Figure 1. *In Vivo* Evidence of T Cell Alterations in Sporadic PD Patients

Postmortem substantia nigra (SN) of sporadic PD patients shows reduced numbers of neuromelanin+ neurons (A and E) compared to control tissue (B and E); examples indicated by stars. In close proximity to neuromelanin+ neurons, CD3+ T cells were detected in PD SN (C and F), but not in control SN, where CD3+ T cells almost exclusively occurred perivascularly (D and F). For quantification, total CD3+ T cells including those juxtaposed to neuromelanin+ neurons as well as perivascular CD3+ cells were counted. *Ex vivo* analysis of circulating T cells of early-disease-stage sporadic PD patients revealed increased frequencies of IL-17-producing CD4+ T cells (Th17 cells) as shown in representative dot plots (G) and confirmed by quantification (H). The frequencies of IFNg- and IL-4-producing T cells (Th1 and Th2 cells, respectively) were not altered between PD cells and controls (H). Scale bars, 50 μm. Experiments were performed using postmortem SN of three PD patients and two controls. The blood analysis was done using 10 sporadic PD patients and 10 controls. Data are shown as means ± SD. *$p < 0.05$ by two-tailed Student's t test. See also Figure S1 and Tables S1 and S2.

lines from sporadic PD cases exhibited, however, limited phenotypes (Sánchez-Danés et al., 2012; Soldner et al., 2009).

To delineate the impact of human T lymphocytes on neurodegeneration in PD, we developed an autologous cell co-culture system of hiPSC-derived MBNs from sporadic PD patients and peripheral blood T lymphocytes from the identical individuals. The physiological relevance in human PD pathology was supported by increased amounts of CD3+ T lymphocytes that were detected in the vicinity of neuromelanin+ neurons in postmortem SN tissues of PD patients. Moreover, elevated frequencies of IL-17-producing CD4+ T cells in the blood of PD patients were associated with an increased *in vitro* ability of T lymphocytes to induce cell death of hiPSC-derived MBNs from PD patients. This effect was driven by the IL-17–IL-17 receptor (IL-17R) signaling and upregulation of its downstream target, nuclear factor kappa-light-chain enhancer of activated B cells (NFκB), and could be rescued by the blockage of IL-17 or IL-17R. Overall, our findings indicate a critical role for IL-17-producing T cells in human PD-associated neuronal cell death.

RESULTS

CD3+ T Lymphocytes Infiltrate the Midbrain of PD Patients

To understand the impact of T lymphocytes in PD, we evaluated the presence of T lymphocytes (CD3+) in the postmortem midbrain of PD patients. As expected, neuromelanin+ cells were significantly reduced in PD (Figures 1A, 1B, and 1E). In PD patients' SN, CD3+ T lymphocytes were significantly increased (6.4 ± 0.9 CD3+ T lymphocytes/mm^2) compared to control (1.9 ± 0.7 CD3+ T lymphocytes/mm^2, Figure 1F). CD3+ T lymphocytes were located close to neuromelanin+ neurons in PD (Figure 1C), but they were almost exclusively present in blood vessels in control SN (Figure 1D). The ratios of T lymphocytes to neuromelanin+ neurons in postmortem SN are about one T lymphocyte per two in PD and per ten in controls of neuromelanin+ neurons (Figures 1E and 1F).

To investigate T lymphocyte subtypes during disease progression, we isolated T lymphocytes from peripheral blood of 10 sporadic PD patients (Hoehn & Yahr: 1-2) and 10 controls (Figure S1A) and analyzed them either in resting state or after *ex vivo* stimulation (Table S1). Significantly increased frequencies of IL-17-producing CD4+ T lymphocytes were detected in PD patients (Figures 1G and 1H), whereas no differences in frequencies both of interferon (IFN)g- and IL-4-producing CD4+ T lymphocytes (Figure 1H) and of CD3+ CD4+ T lymphocytes (Figure S1B and Table S1) were observed.

The expression of surface markers in resting and *ex vivo*-stimulated T lymphocytes indicated reduced numbers of

CD4+ CD25+ T lymphocytes in PD samples. Of note, significantly higher frequencies of CD178+ (Fas Ligand) within stimulated CD4+ and CD8+ T lymphocytes were observed in PD patients (Table S1), indicating an upregulation of pathways regulating cell death. Frequencies of CD4+, CD8+, CD95+ (Fas Receptor), and CD54+ (an adhesion molecule, ICAM-1) T lymphocytes and expression of dopamine receptors (DR1-5) were unchanged in resting condition and after stimulation (Table S1). No significant correlation between the amount of dopaminergic medication (Levodopa equivalent daily dose [LEDD] (Tomlinson et al., 2010)) and frequencies of IL-17-producing CD4+ T lymphocytes in PD patients was found (Figure S1C).

T Lymphocytes Induce Cell Death in Autologous hiPSC-Derived MBNs from PD Patients

To understand how T lymphocytes contribute to neurodegeneration in PD, we established a human autologous co-culture of T lymphocytes with PD patient hiPSC-derived MBNs. MBNs were generated from sporadic PD patients in an early disease stage (Hoehn & Yahr: 1-2) and age- and sex-matched controls (Table S2) via reprogramming of fibroblasts to hiPSCs (Figure S2A). We analyzed hiPSC pluripotency and differentiated hiPSCs into MBNs via an intermediate step of neural precursor cells generated by the addition of small molecules (small molecule neural precursor cells [smNPCs], Figures S2B and S2C) (Reinhardt et al., 2013). Neuronal differentiation was comparably effective in all hiPSC lines and MBNs expressed β-3-tubulin (TUBB3, pan neural marker), tyrosine hydroxylase (TH; about 15% TH+ neurons), inward rectifying potassium channel (Girk2, gene *KCNJ6*, midbrain dopaminergic [DA] neuronal marker), and the nuclear receptor-related 1 protein (Nurr1, gene *NR4A2*, DA neuronal marker) at comparable levels and were functional (Figures S2C–S2E). Next, we co-cultured hiPSC-derived MBNs with the respective autologous CD3+ T lymphocytes following optimization of co-culture conditions and cell ratios (Figure S3A). Unless indicated, co-culture experiments were performed with the ratio of one T lymphocyte to one MBN, within the range of the calculated ratio in postmortem tissues (Figures 1E and 1F). The co-culture of MBNs with *ex vivo* polyclonally activated autologous T lymphocytes using CD3 CD28 dynabeads (paradigm: Figure 2A) resulted in significantly increased neuronal cell death in the PD group (assessed by activated Caspase 3 [aCASP3]/TUBB3 double-positive neurons, Figures 2B and 2C; and by TUNEL/TUBB3 double-positive cells, Figure 2D). The ratio of one T lymphocyte to ten neurons also led to a significant increase in neuronal cell death in PD (Figure 2C). Neuronal cell death was unchanged in PD and control without the addition of T lymphocytes (Figures 2B–2D). Accordingly, a prolonged co-culture time of up to 10 days was not able to induce increased neuronal cell death in control neurons (Figure S3B), excluding the possibility of a delayed response of control neurons to T lymphocytes.

In PD co-cultures of T lymphocytes and hiPSC-derived MBNs, significantly increased neuronal death of both TH+ and TH− neurons was detected with a higher cell death rate in TH+ neurons (Figures 2E and 2F). A significantly reduced TH neurite length was found after co-culture with T lymphocytes in both PD and control TH+ neurons (Figure 2G).

T Lymphocytes Induce Cell Death of PD hiPSC-Derived MBNs by IL-17–IL-17R Signaling

To test if PD patient hiPSC-derived MBNs were more susceptible to PD-specific T lymphocytes, we co-cultured PD hiPSC-derived neurons with control T lymphocytes or control hiPSC-derived neurons with PD T lymphocytes (Figure 2H). PD hiPSC-derived neurons showed no increase in cell death levels in co-culture with control T lymphocytes; nor did PD T lymphocytes induce pronounced cell death of control hiPSC-derived neurons (Figure 2I). These results indicate a neurotoxic capacity of PD T lymphocytes toward PD-related neurons, suggesting that a PD-specific co-culture was necessary for an increase in T lymphocyte-induced neuronal death. To test the potential role of major histocompatibility complex (MHC) class I mismatches in allogeneic T cell:neuron co-cultures, we stained hiPSC-derived neurons from autologous and allogeneic co-cultures as well as untreated hiPSC-derived neurons for MHC class I. We detected very faint MHC class I levels in hiPSC-derived neurons in all of the three conditions, whereas positive MHC class I staining was found in Lipopolysaccharides (LPS)-treated astrocytes, which were used as a positive control (Figure S3C).

To determine the impact of Th17 lymphocytes on neurodegeneration in PD, we analyzed cytokines in the supernatants of hiPSC-based co-cultures (Figure 3A) and found increased levels of IL-17 in PD co-cultures (Figure 3B). In addition, increased levels of the pro-inflammatory cytokines tumor necrosis factor (TNF)a, IL-1b, and IL-6, known to be elevated in PD, were found in the supernatant of PD hiPSC-based co-cultures (data not shown). Gene expression of the respective cytokine receptors indicated that the IL-17R was significantly upregulated in hiPSC-derived neurons from PD patients compared to controls after 3 days of co-culture (Figure 3C). This finding was further supported by immunostaining and western blot analysis, which revealed increased expression of IL-17R in hiPSC-derived neurons from PD patients after stimulation with IL-17 (Figures 3D and 3E). The expression of genes encoding the TNFa receptor (TNFaR) and IL-1 receptor (IL-1R) was not altered (data not shown). As was now predicted, we detected IL-17R expression in neuromelanin+ neurons in the postmortem SN tissues from PD patients (Figure S4A), confirming our cell culture findings *in vivo* in human PD brains.

IL-17, added to hiPSC-derived MBNs for 3 days (Figure 3F), led to increased neuronal cell death in hiPSC-derived MBNs from PD patients, but not in controls (Figure 3G). Thus, we demonstrated that IL-17 is capable of inducing increased cell death in hiPSC-derived neurons from PD patients and that these are more susceptible to IL-17-induced cell death. Moreover, IL-17 released from T lymphocytes induces cell death in hiPSC-derived MBNs from PD patients, possibly by upregulating neuronal IL-17R expression. We hypothesized that blockage of IL-17 or IL-17R might prevent T lymphocyte-induced neuronal death. Therefore, IL-17- or IL-17R-neutralizing antibodies were added to the hiPSC-derived MBNs prior to co-culture with autologous T lymphocytes (Figure 3H). Both IL-17 and IL-17R blockages were able to fully rescue the T lymphocyte-induced cell death of the total neuronal population (Figure 3I) and the TH+ neurons (data not shown). Remarkably, secukinumab (Cosentyx), an FDA-approved humanized anti-IL-17 antibody

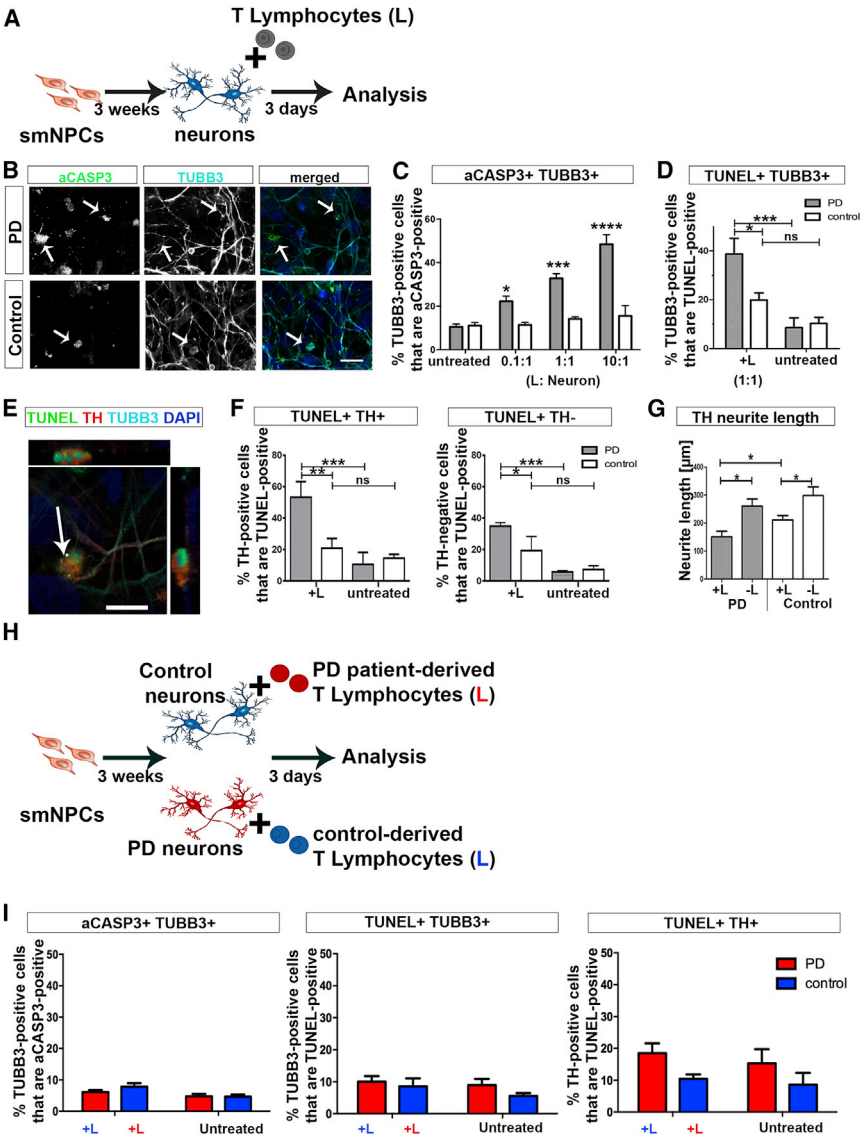

Figure 2. Increased Cell Death in PD hiPSC-Derived Neurons after Co-culture with Autologous T Lymphocytes

hiPSC-derived midbrain neurons (neurons) were co-cultured with autologous T lymphocytes (L) isolated from peripheral blood for 3 days (A). Increased numbers of activated Caspase 3 (aCASP3)+/β-3-tubulin (TUBB3)+ neurons were found in PD co-cultures but not in control, as shown in representative immunofluorescence images (B, double-positive cells indicated by arrows) and quantified in (C) for different T cell:neuron ratios compared to untreated conditions. The enhanced cell death rate was confirmed by increased numbers of TUNEL+/TUBB3+ neurons in PD when co-cultured with T lymphocytes at the 1:1 ratio (D, +L). Increased cell death was also found in TH+ and TH− hiPSC-derived neurons in PD compared to control determined by increased numbers of TUNEL+/TH+ and TUNEL+/TH− neurons, respectively (E and F, +L). TH+ neurons had reduced neurite length after co-culture with T lymphocytes in PD and controls (+L) (G). Non-autologous co-culture of PD-derived T lymphocytes (red L) with control hiPSC-derived midbrain neurons (blue) or vice versa (H) did not induce any neuronal cell death (I). Neuronal cell death was determined via staining for aCASP3 or TUNEL of either whole neuronal population (TUBB3+) or dopaminergic neurons (TH+). Scale bars, 50 µm in (B), 20 µm in (E). Experiments were performed using two hiPSC clones for each of three patients/controls (n = 6 per group). Data are shown as means ± SD. *p < 0.05, **p < 0.01, ***p < 0.001, ****p < 0.0001 by one-way (in D, F, and G) and two-way (in C) ANOVA and Sidak or Tukey tests for multiple comparisons. ns, not significant. See also Figures S2 and S3 and Table S2.

clinically used in psoriasis treatment, was also able to rescue the T lymphocyte-induced neuronal death in PD hiPSC-based neuronal co-cultures (Figure 3I). Hence, T lymphocytes induced neuronal death via IL-17 bound to the IL-17R and thus activated downstream cell death signaling.

Since hiPSC-derived neuronal cultures contain low numbers of astrocytes (5%–10%), we tested the possibility that the effect of IL-17 on human neurons was transduced by astrocytes. IL-17 was added to human primary astrocytes and did not change the IL-17R and IL-17 gene expression (Figure S4B).

NFκB Signaling Is Activated by IL-17 Signaling in hiPSC-Derived MBNs from PD Patients

To obtain insights into the mechanisms by which IL-17 leads to MBN death in PD, we performed deep RNA sequencing (RNA-seq) of IL-17-treated PD and control hiPSC-derived neurons (Figure 4A). Upon IL-17 treatment only 17 genes were found to be dysregulated in controls, but 125 genes were dysregulated in hiPSC-derived MBNs from PD patients (DESeq2 analysis, adj. $p < 0.05$, log2FC [fold change] > 1, mean RPKM [reads per kilobase per million mapped reads] of gene > 1), with minor overlap between regulated genes in hiPSC-derived MBNs from control and PD patients (Figure 4B). The 125 IL-17-dependent genes in PD hiPSC-derived neurons separated the treated from untreated PD hiPSC-derived neuronal samples using an unsupervised, hierarchical clustering applying a Euclidean distance metric (Figure 4C). When the exact same 125 genes were applied to the control samples, no clustering of IL-17-treated versus untreated hiPSC-derived neuronal samples by the same method could be observed (Figure S4C), indicative of a PD-specific IL-17-inducible gene expression pattern.

Gene expression changes upon IL-17 signaling are accomplished by activation of different transcription factors (TFs), including CEBPB, NFκB, and AP1 (heterodimer of cFos and cJun). By analyzing the TF binding sites (TFBSs) of the three abovementioned TF in promoters of genes regulated by IL-17 in hiPSC-derived neurons from PD patients, we found that only NFκB sites computed a significant TFBS enrichment in genes induced, but not repressed, by IL-17 (Figure 4D),

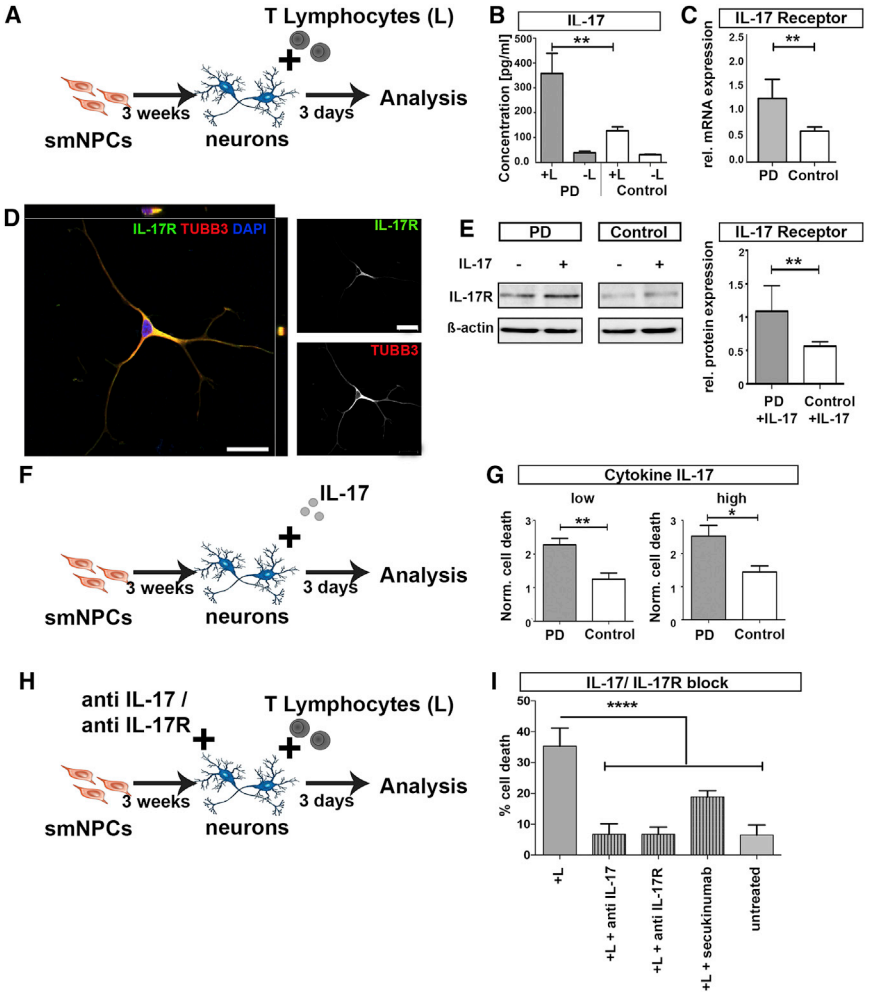

Figure 3. IL-17-Mediated Cell Death in PD hiPSC-Derived Neurons

After co-culture of hiPSC-derived neurons with autologous T lymphocytes (L) for 3 days (A), increased amounts of IL-17 were detected in the supernatants of PD co-cultures (B). Increased expression of the IL-17 receptor (IL-17R) was detected after 3 days of PD co-culture on mRNA (C) and protein levels (D and E). When treating hiPSC-derived neurons with either low (concentration corresponding to the concentration in the co-culture supernatants) or high (10-fold higher than low) concentrations of IL-17 (F), PD neurons underwent increased cell death as determined by the staining for aCASP3 and normalized to untreated neurons (G). Treatment of PD hiPSC-derived neurons with IL-17 or IL-17R neutralizing antibodies or the FDA-approved anti-IL-17 antibody secukinumab directly prior to the 3 day co-culture with autologous T lymphocytes (H) led to a reduction in T cell-induced neuronal death (+L) comparable to the cell death levels of neurons cultured without T lymphocytes (untreated) (I). Scale bar, 50 μm. Experiments were performed with two hiPSC clones for each of the three patients/controls (n = 6 per group). Data are shown as means ± SD. *p < 0.05, **p < 0.01, ****p < 0.0001 by one-way ANOVA and Sidak Test for multiple comparisons. See also Figures S4A and S4B.

suggesting an important role for NFκB activation in IL-17-induced signaling in PD hiPSC-derived neurons. Quantitative reverse transcription (qRT)-PCR confirmed an increased expression of *STK36*, *SLC9A3*, *ABCA7*, and *PCSK4* genes, found to be upregulated upon IL-17 treatment in hiPSC-derived neurons from PD patients by RNA-seq with enrichment of NFκB TFBSs (Figure S4D).

Western blot analysis for the p65 and p50 components of the NFκB heterodimer, which is typically involved in the inflammatory response, revealed comparable levels of p65 in the cytoplasmic fraction of untreated hiPSC-derived neurons from PD patients and controls, demonstrating similar baseline levels (Figure 4E). Treatment with IL-17 resulted in a significant upregulation of cytoplasmic and nuclear p65 and p50 levels in hiPSC-derived neurons from PD patients, but not in controls (Figures 4F–4I), indicative of activated NFκB signaling. Additionally, we found upregulation of Act1 in PD, but not control, hiPSC-derived neurons after IL-17 treatment (Figure 4J), which is a downstream target of IL-17R signaling and upstream to NFκB, further supporting our hypothesis. Thus, we propose a model in which NFκB activation might be the central pathway involved in IL-17-induced neuronal cell death following T lymphocyte interaction in PD (Figure S4E).

DISCUSSION

Neuroinflammation is contributing to neurodegeneration in sporadic PD (Hirsch et al., 2012; Ransohoff, 2016). However, the role of adaptive immune cells in PD pathogenesis remains unsolved. Here, we provide *in vivo* and *in vitro* data to delineate an important contribution of T lymphocytes in human PD pathology.

In contrast to the initial dogma that peripheral immune cells are unable to enter the CNS, it is now established that peripheral immune cells infiltrate the CNS under pathological conditions and may trigger neurodegeneration (Mosley et al., 2012). T lymphocytes infiltrate into the CNS in neurodegenerative disease either due to blood-brain barrier dysfunction (Kortekaas et al., 2005) or via the choroid plexus (Schwartz and Baruch, 2014). Indeed, in PD postmortem tissue, T lymphocytes were shown to be present in the CNS (Brochard et al., 2009), which is also confirmed by our *in vivo* data: increased numbers of CD3+ T lymphocytes in close proximity to neuromelanin+ neurons in postmortem SN tissues of PD patients point to the relevance of T lymphocytes for PD pathology. The calculated cell ratio in PD SN in both studies was one T lymphocyte per two neuromelanin+ neurons and in the range of the cell ratios (1:1−1:10) used in the human autologous co-culture model in our study. This ratio might result from a loss of neuromelanin+ DA neurons and increased T lymphocyte infiltration into the CNS in PD.

By implementing an innovative, patient hiPSC-based co-culture model, we delineated a specific role of T lymphocytes in neuronal cell death in sporadic PD. Patient-specific T

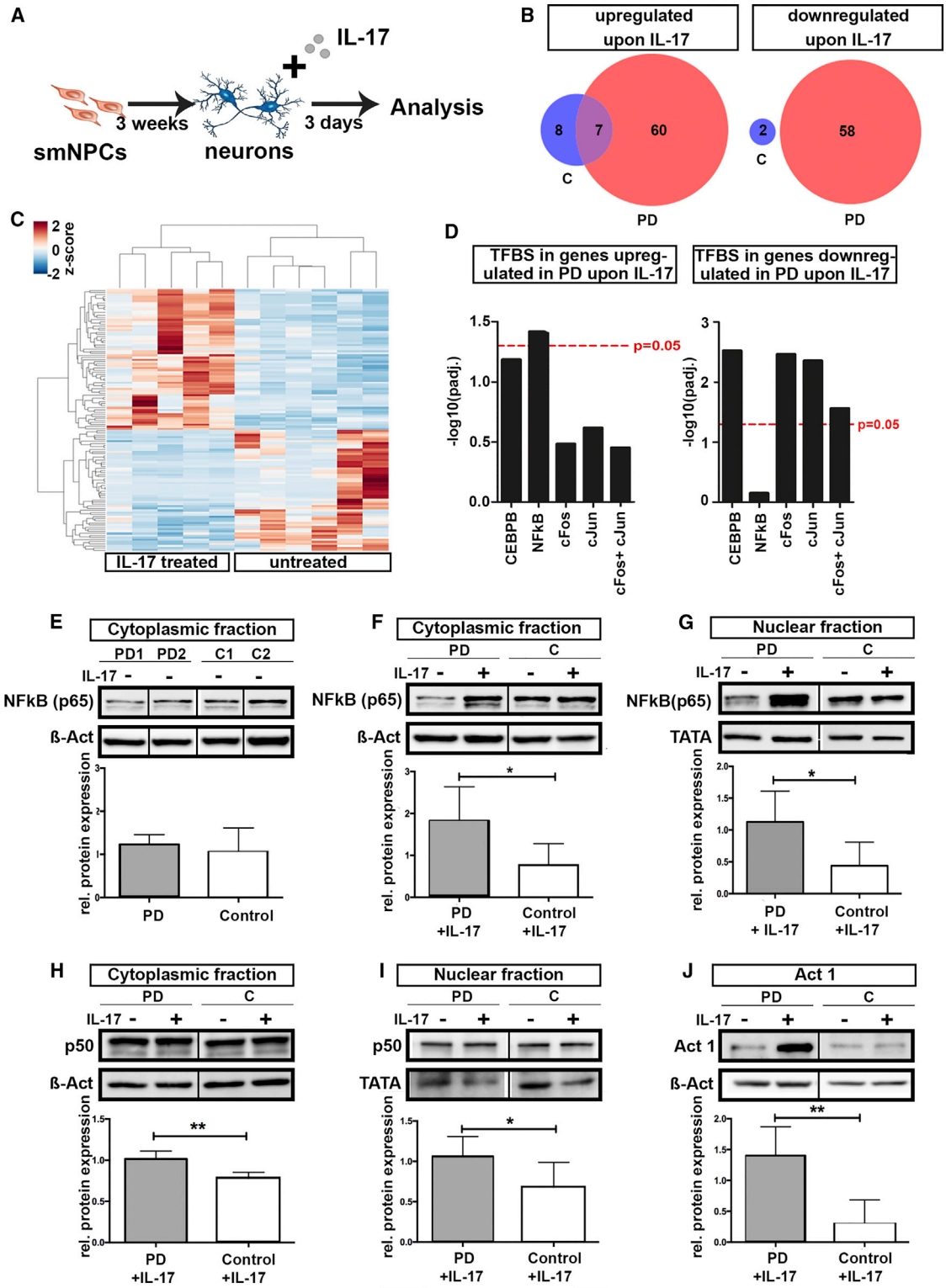

Figure 4. NFκB Activation in PD Patient hiPSC-Derived Neurons after IL-17 Treatment

RNA sequencing analysis was performed in IL-17-treated and untreated hiPSC-derived neurons (A). Gene expression changes in control (C) and PD neurons upon IL-17 treatment were determined by DESeq2 analysis and illustrated in Venn diagrams showing numbers of significantly differentially regulated genes (defined as having an adjusted $p < 0.05$, log2FoldChange [FC] > 1, and mean reads per kilobase per million > 1) (B). A heatmap represents unsupervised hierarchical clustering based on the expression of the 125 differentially regulated genes in PD samples, which separates IL-17-treated and -untreated PD samples. Benjamini-Hochberg corrected p values representing the enrichment significance of transcription factor binding sites (TFBSs) in the promoters of the 125

(legend continued on next page)

lymphocytes led to an increased cell death of hiPSC-derived MBNs from PD patients. Both hiPSC-derived TH+ and TH− MBNs were affected by T lymphocytes in PD with a higher cell death rate in the TH+ population. This indicates that all midbrain neuronal populations are affected by activated T lymphocytes, but DA neurons might be slightly more vulnerable, suggesting that there might be a slight neurotransmitter phenotype specificity of the immune response. In accordance with this, in the 1-methyl-4-phenyl-1,2,3,6-tetrahydropyridine (MPTP) mouse model of PD, CNS-infiltrating T lymphocytes were responsible for nigrostriatal neuronal cell death (Brochard et al., 2009). Also in line with this, in a human cell culture system, increased susceptibility of DA neurons to a T lymphocyte-mediated cytotoxic attack was reported (Cebrián et al., 2014). This effect was mostly mediated by IFNg, which was shown to induce the expression of MHC class I in human stem cell-derived DA neurons (Cebrián et al., 2014). In our experiments, IFNg levels were not altered between control and PD patients and in our hiPSC-derived neurons, MHC class I expression was detectable at very faint levels, comparable in untreated and autologous or allogeneic co-cultured neurons. Our data show that PD patient hiPSC-derived midbrain neuronal cell death could be strongly linked to IL-17-producing CD4+ T lymphocytes. This suggests that, in addition to neuronal vulnerability to CD8+ cytotoxic T lymphocytes (Cebrián et al., 2014), CD4+ T cells are involved in human PD pathology. Importantly, both studies independently showed the particular susceptibility of MBNs to the effects of adaptive immune cells in a human *in vitro* model. Notably, a majority of hiPSC-based studies describe cellular neuronal phenotypes of monogenic PD cases (Avior et al., 2016; Imaizumi et al., 2012; Nguyen et al., 2011; Ohta et al., 2015; Ryan et al., 2013; Shaltouki et al., 2015). In sporadic PD, reduced numbers of neurites and neurite arborization were only present in hiPSC-based models following long-term neuronal culture of 75 day cultures (Sánchez-Danés et al., 2012). This indicates the necessity to add further stressors to the intrinsic susceptibility to delineate disease-specific pathology in sporadic PD. Here, we describe how activated peripheral immune cells impair the survival of MBNs derived from hiPSCs of sporadic PD patients to a greater extent than controls. This suggests the susceptibility of MBNs to the effects of adaptive immune cells.

Mechanistically, we show that T lymphocyte-induced neuronal cell death in PD is mediated by IL-17 signaling via IL-17R. This results in downstream activation of NFκB. In accordance with this, previous studies of postmortem SN of PD patients detected increased levels of nuclear NFκB (Soós et al., 2004). Notably, increased expression of IL-17R in PD patient hiPSC-derived neurons might underlie the specific responsiveness of these neurons to IL-17 and to PD-derived T lymphocytes, which comprise higher frequencies of IL-17 producers. Moreover, rescue of the T lymphocyte-induced neuronal cell death by blockage of either IL-17 or IL-17R, or by using the FDA-approved drug secukinumab, is further indication of specific IL-17-induced cell death in hiPSC-derived neurons from PD patients and directs us toward new potential immunotherapeutic approaches for PD.

Previous studies investigating immune cell populations in the blood of PD patients resulted in inconclusive findings (reviewed in Sommer et al., 2017), probably due to divergent experimental setups. The approach undertaken here was to analyze isolated T lymphocytes *ex vivo*, revealing significantly increased frequencies of IL-17-producing CD4+ T lymphocytes (Th17 cells) in the peripheral blood of sporadic PD patients and suggesting that the pathogenesis of sporadic PD might be accompanied by Th17 cell-driven systemic inflammation. CNS-infiltrating Th17 cells were shown to induce neurodegeneration in the MPTP mouse model by direct interaction with neurons via the adhesion molecules LFA-1 and ICAM-1 expressed on Th17 cells and neurons, respectively (Kawanokuchi et al., 2008; Liu et al., 2016). While this data favors a contact-dependent signaling by adhesion molecules in a mouse model, our human data demonstrates that the IL-17R is expressed and modulated in human neurons, permitting cytokine-dependent signaling of Th17 cells.

In summary, we propose that autologous IL-17-producing CD4+ T cells cause neuronal cell death in sporadic PD. Our data support a model of neuroinflammation in PD, driven by adaptive immune cells, in which Th17 cell-released IL-17 binds to IL-17R expressed on MBNs, inducing downstream signaling by upregulation of NFκB. The role of glial cells in Th17-mediated neuronal cell death in PD adds additional complexity. Autologous co-culture experiments with the addition of hiPSC-derived microglia (Muffat et al., 2016) could clarify their potential involvement in Th17-induced neuronal cell death in PD. In line with this, α-synuclein-activated microglia were shown to induce MHC class I expression on neurons (Cebrián et al., 2014), indicating that activated microglia might mediate an effect of peripheral immune cells by priming ventral MBNs.

Overall, our findings propose a specific role for T lymphocytes in mediating neuronal cell death in sporadic PD. The elevated presence of Th17 cells in the blood of PD patients might explain increased toxicity of PD-derived T lymphocytes for hiPSC-derived neurons from PD patients mediated by IL-17. Th17 cells are key players in autoimmune diseases like MS or rheumatoid arthritis, and their possible involvement in PD might revise our understanding of how PD neurodegeneration might be promoted by systemic inflammation driven by adaptive immunity.

STAR★METHODS

Detailed methods are provided in the online version of this paper and include the following:

- KEY RESOURCES TABLE
- CONTACT FOR REAGENT AND RESOURCE SHARING

differentially regulated genes in PD hiPSC-derived neurons upon IL-17 treatment is shown in (D). −log10 (padj.) indicates −log10 of the adjusted p values; dashed red line represents a significance threshold of p = 0.05. Western blot analysis revealed comparable levels of NFκB (p65) in the cytoplasmic fraction of untreated PD and control hiPSC-derived neurons (E). After IL-17 treatment, increased levels of cytoplasmic (F) and nuclear (G) NFκB p65 protein were found in PD, but not in control neurons. The p50 protein level was significantly increased in the cytoplasmic (H) and nuclear (I) fractions in PD hiPSC-derived neurons following IL-17 treatment. Act1 protein levels were increased in PD hiPSC-derived neurons following IL-17 treatment (J). Experiments were performed with two hiPSC clones for each of three patients/controls (n = 6 per group). Data are shown as means ± SD. *p < 0.05, **p < 0.01 by Student's t test. See also Figures S4C–S4E.

SUPPLEMENTAL INFORMATION

Supplemental Information includes three tables and four figures and can be found with this article online at https://doi.org/10.1016/j.stem.2018.06.015.

ACKNOWLEDGMENTS

This work is dedicated to our patients. We thank Michaela Farrell, Sonja Plötz, and Holger Wend for excellent technical support; Ralf Linker, Georg Schett, Katharina Brandl, Markus Schulze, and Nina Henriette Uhlenhaut for help and critical input. We thank M.L. Gage for editorial comments. Secukinumab was kindly provided by Gerhard Krönke. We received human postmortem samples from the Netherlands Brain Bank (NBB #1043). This study was funded by the Bavarian Ministry of Education and Culture, Science, and the Arts in the framework of the Bavarian Research Network Induced Pluripotent Stem Cells ForIPS. Additional support for this study came from the German Federal Ministry of Education and Research (BMBF: 01GQ113, 01GM1520A, 01EK1609B), the DFG funded research training group GRK2162 (to B.W. and J.W.) and DFG grant 410/45-1 FUGG, the Interdisciplinary Centre for Clinical Research (University Hospital of Erlangen E25 [B.W.], J66 [E.E.], and J51 [F.M.]), the Bavarian Ministry of Education and Culture, Science and the Arts in the framework of the Bavarian Molecular Biosystems Research Network ("BioSysNet") and the Core Unit Cell Sorting and Immunomonitoring (UK Erlangen). Additional support was provided by the JPB Foundation, the Mathers Foundation, and the Lookout Foundation. Florian Krach is funded by the Bavaria California Technology Center (BaCaTec).

AUTHOR CONTRIBUTIONS

A.S. and I.P. designed and performed the experiments, analyzed the data, and wrote the manuscript; T.F. and D.G. performed the experiments; J.W., F.H.G., Z.K., and F.M. provided the patient material; F.K. and G.W.Y. performed the RNA-seq analysis; E.E. and M.M. performed the electrophysiology; J.G., M.J.R., and W.X. provided technical support and analyzed the data; and I.P. and B.W. directed the entire study, designed the experiments, analyzed the data, and wrote the manuscript.

DECLARATION OF INTERESTS

The authors declare that they have no competing interests.

Received: May 30, 2017
Revised: February 26, 2018
Accepted: June 19, 2018
Published: July 5, 2018

REFERENCES

Avior, Y., Sagi, I., and Benvenisty, N. (2016). Pluripotent stem cells in disease modelling and drug discovery. Nat. Rev. Mol. Cell Biol. *17*, 170–182.

Baba, Y., Kuroiwa, A., Uitti, R.J., Wszolek, Z.K., and Yamada, T. (2005). Alterations of T-lymphocyte populations in Parkinson disease. Parkinsonism Relat. Disord. *11*, 493–498.

Bas, J., Calopa, M., Mestre, M., Molleví, D.G., Cutillas, B., Ambrosio, S., and Buendia, E. (2001). Lymphocyte populations in Parkinson's disease and in rat models of parkinsonism. J. Neuroimmunol. *113*, 146–152.

Borgs, L., Peyre, E., Alix, P., Hanon, K., Grobarczyk, B., Godin, J.D., Purnelle, A., Krusy, N., Maquet, P., Lefebvre, P., et al. (2016). Dopaminergic neurons differentiating from LRRK2 G2019S induced pluripotent stem cells show early neuritic branching defects. Sci. Rep. *6*, 33377.

Brochard, V., Combadière, B., Prigent, A., Laouar, Y., Perrin, A., Beray-Berthat, V., Bonduelle, O., Alvarez-Fischer, D., Callebert, J., Launay, J.M., et al. (2009). Infiltration of CD4+ lymphocytes into the brain contributes to neurodegeneration in a mouse model of Parkinson disease. J. Clin. Invest. *119*, 182–192.

Byers, B., Cord, B., Nguyen, H.N., Schüle, B., Fenno, L., Lee, P.C., Deisseroth, K., Langston, J.W., Pera, R.R., and Palmer, T.D. (2011). SNCA triplication Parkinson's patient's iPSC-derived DA neurons accumulate α-synuclein and are susceptible to oxidative stress. PLoS ONE *6*, e26159.

Cebrián, C., Zucca, F.A., Mauri, P., Steinbeck, J.A., Studer, L., Scherzer, C.R., Kanter, E., Budhu, S., Mandelbaum, J., Vonsattel, J.P., et al. (2014). MHC-I expression renders catecholaminergic neurons susceptible to T-cell-mediated degeneration. Nat. Commun. *5*, 3633.

Consortium, E.P.; ENCODE Project Consortium (2012). An integrated encyclopedia of DNA elements in the human genome. Nature *489*, 57–74.

Cutforth, T., DeMille, M.M., Agalliu, I., and Agalliu, D. (2016). CNS autoimmune disease after *Streptococcus pyogenes* infections: animal models, cellular mechanisms and genetic factors. Future Neurol. *11*, 63–76.

Dendrou, C.A., Fugger, L., and Friese, M.A. (2015). Immunopathology of multiple sclerosis. Nat. Rev. Immunol. *15*, 545–558.

Giuliani, F., Goodyer, C.G., Antel, J.P., and Yong, V.W. (2003). Vulnerability of human neurons to T cell-mediated cytotoxicity. J. Immunol. *171*, 368–379.

Havlicek, S., Kohl, Z., Mishra, H.K., Prots, I., Eberhardt, E., Denguir, N., Wend, H., Plötz, S., Boyer, L., Marchetto, M.C., et al. (2014). Gene dosage-dependent rescue of HSP neurite defects in SPG4 patients' neurons. Hum. Mol. Genet. *23*, 2527–2541.

Hirsch, E.C., Vyas, S., and Hunot, S. (2012). Neuroinflammation in Parkinson's disease. Parkinsonism Relat. Disord. *18* (*Suppl 1*), S210–S212.

Imaizumi, Y., Okada, Y., Akamatsu, W., Koike, M., Kuzumaki, N., Hayakawa, H., Nihira, T., Kobayashi, T., Ohyama, M., Sato, S., et al. (2012). Mitochondrial dysfunction associated with increased oxidative stress and α-synuclein accumulation in PARK2 iPSC-derived neurons and postmortem brain tissue. Mol. Brain *5*, 35.

Kapeli, K., Pratt, G.A., Vu, A.Q., Hutt, K.R., Martinez, F.J., Sundararaman, B., Batra, R., Freese, P., Lambert, N.J., Huelga, S.C., et al. (2016). Distinct and shared functions of ALS-associated proteins TDP-43, FUS and TAF15 revealed by multisystem analyses. Nat. Commun. *7*, 12143.

Kawanokuchi, J., Shimizu, K., Nitta, A., Yamada, K., Mizuno, T., Takeuchi, H., and Suzumura, A. (2008). Production and functions of IL-17 in microglia. J. Neuroimmunol. *194*, 54–61.

Kortekaas, R., Leenders, K.L., van Oostrom, J.C., Vaalburg, W., Bart, J., Willemsen, A.T., and Hendrikse, N.H. (2005). Blood-brain barrier dysfunction in parkinsonian midbrain in vivo. Ann. Neurol. *57*, 176–179.

Lee, G., and Studer, L. (2010). Induced pluripotent stem cell technology for the study of human disease. Nat. Methods *7*, 25–27.

Liu, Z., Huang, Y., Cao, B.B., Qiu, Y.H., and Peng, Y.P. (2016). Th17 Cells Induce Dopaminergic Neuronal Death via LFA-1/ICAM-1 Interaction in a Mouse Model of Parkinson's Disease. Mol. Neurobiol. *54*, 7762–7776.

Mosley, R.L., Hutter-Saunders, J.A., Stone, D.K., and Gendelman, H.E. (2012). Inflammation and adaptive immunity in Parkinson's disease. Cold Spring Harb. Perspect. Med. *2*, a009381.

Muffat, J., Li, Y., Yuan, B., Mitalipova, M., Omer, A., Corcoran, S., Bakiasi, G., Tsai, L.H., Aubourg, P., Ransohoff, R.M., and Jaenisch, R. (2016). Efficient derivation of microglia-like cells from human pluripotent stem cells. Nat. Med. *22*, 1358–1367.

Nguyen, H.N., Byers, B., Cord, B., Shcheglovitov, A., Byrne, J., Gujar, P., Kee, K., Schüle, B., Dolmetsch, R.E., Langston, W., et al. (2011). LRRK2 mutant iPSC-derived DA neurons demonstrate increased susceptibility to oxidative stress. Cell Stem Cell *8*, 267–280.

Ohta, E., Nihira, T., Uchino, A., Imaizumi, Y., Okada, Y., Akamatsu, W., Takahashi, K., Hayakawa, H., Nagai, M., Ohyama, M., et al. (2015). I2020T mutant LRRK2 iPSC-derived neurons in the Sagamihara family exhibit increased Tau phosphorylation through the AKT/GSK-3β signaling pathway. Hum. Mol. Genet. *24*, 4879–4900.

Ransohoff, R.M. (2016). How neuroinflammation contributes to neurodegeneration. Science *353*, 777–783.

Reinhardt, P., Glatza, M., Hemmer, K., Tsytsyura, Y., Thiel, C.S., Höing, S., Moritz, S., Parga, J.A., Wagner, L., Bruder, J.M., et al. (2013). Derivation and expansion using only small molecules of human neural progenitors for neurodegenerative disease modeling. PLoS ONE *8*, e59252.

Reynolds, A.D., Stone, D.K., Hutter, J.A., Benner, E.J., Mosley, R.L., and Gendelman, H.E. (2010). Regulatory T cells attenuate Th17 cell-mediated nigrostriatal dopaminergic neurodegeneration in a model of Parkinson's disease. J. Immunol. *184*, 2261–2271.

Ryan, S.D., Dolatabadi, N., Chan, S.F., Zhang, X., Akhtar, M.W., Parker, J., Soldner, F., Sunico, C.R., Nagar, S., Talantova, M., et al. (2013). Isogenic human iPSC Parkinson's model shows nitrosative stress-induced dysfunction in MEF2-PGC1α transcription. Cell *155*, 1351–1364.

Sánchez-Danés, A., Richaud-Patin, Y., Carballo-Carbajal, I., Jiménez-Delgado, S., Caig, C., Mora, S., Di Guglielmo, C., Ezquerra, M., Patel, B., Giralt, A., et al. (2012). Disease-specific phenotypes in dopamine neurons from human iPS-based models of genetic and sporadic Parkinson's disease. EMBO Mol. Med. *4*, 380–395.

Schwartz, M., and Baruch, K. (2014). The resolution of neuroinflammation in neurodegeneration: leukocyte recruitment via the choroid plexus. EMBO J. *33*, 7–22.

Shaltouki, A., Sivapatham, R., Pei, Y., Gerencser, A.A., Momčilović, O., Rao, M.S., and Zeng, X. (2015). Mitochondrial alterations by PARKIN in dopaminergic neurons using PARK2 patient-specific and PARK2 knockout isogenic iPSC lines. Stem Cell Reports *4*, 847–859.

Soldner, F., Hockemeyer, D., Beard, C., Gao, Q., Bell, G.W., Cook, E.G., Hargus, G., Blak, A., Cooper, O., Mitalipova, M., et al. (2009). Parkinson's disease patient-derived induced pluripotent stem cells free of viral reprogramming factors. Cell *136*, 964–977.

Sommer, A., Fadler, T., Dorfmeister, E., Hoffmann, A.C., Xiang, W., Winner, B., and Prots, I. (2016). Infiltrating T lymphocytes reduce myeloid phagocytosis activity in synucleinopathy model. J. Neuroinflammation *13*, 174.

Sommer, A., Winner, B., and Prots, I. (2017). The Trojan horse - neuroinflammatory impact of T cells in neurodegenerative diseases. Mol. Neurodegener. *12*, 78.

Soós, J., Engelhardt, J.I., Siklós, L., Havas, L., and Majtényi, K. (2004). The expression of PARP, NF-kappa B and parvalbumin is increased in Parkinson disease. Neuroreport *15*, 1715–1718.

Stevens, C.H., Rowe, D., Morel-Kopp, M.C., Orr, C., Russell, T., Ranola, M., Ward, C., and Halliday, G.M. (2012). Reduced T helper and B lymphocytes in Parkinson's disease. J. Neuroimmunol. *252*, 95–99.

Sulzer, D., Alcalay, R.N., Garretti, F., Cote, L., Kanter, E., Agin-Liebes, J., Liong, C., McMurtrey, C., Hildebrand, W.H., Mao, X., et al. (2017). T cells from patients with Parkinson's disease recognize α-synuclein peptides. Nature *546*, 656–661.

Takahashi, K., Tanabe, K., Ohnuki, M., Narita, M., Ichisaka, T., Tomoda, K., and Yamanaka, S. (2007). Induction of pluripotent stem cells from adult human fibroblasts by defined factors. Cell *131*, 861–872.

Tomlinson, C.L., Stowe, R., Patel, S., Rick, C., Gray, R., and Clarke, C.E. (2010). Systematic review of levodopa dose equivalency reporting in Parkinson's disease. Mov. Disord. *25*, 2649–2653.

STAR★METHODS

KEY RESOURCES TABLE

REAGENT or RESOURCE	SOURCE	IDENTIFIER
Antibodies		
CD3 FITC	Miltenyi	130-080-401, RRID: AB_244231
CD4 PE	Miltenyi	130-098-134, RRID: AB_2660468
CD8 PE	Miltenyi	130-091-084, RRID: AB_244338
CD8 APC	Miltenyi	130-091-076, RRID: AB_244335
CD19 APC	Miltenyi	130-098-069, RRID: AB_2661287
CD25 FITC	Miltenyi	130-104-323, RRID: AB_2661152
CD54 APC	Miltenyi	130-103-840, RRID: AB_2658697
CD95 APC	Miltenyi	130-092-417, RRID: AB_871700
CD127 PE	Miltenyi	130-094-889, RRID: AB_10828927
CD178 APC	Miltenyi	130-096-458, RRID: AB_10827748
IFNg FITC	Miltenyi	130-091-641, RRID: AB_244194
IL-2 PE	Miltenyi	130-091-646, RRID: AB_244197
IL-4 PE	Miltenyi	130-091-647, RRID: AB_615125
IL-10 PE	Miltenyi	130-096-043, RRID: AB_10828152
IL-17A PE	Miltenyi	130-094-521, RRID: AB_10827702
Tra-1-60 FITC	BioLegend	330614, RRID: AB_2119064
Oct 3/4	Santa Cruz	sc-5279, RRID: AB_628051
Nanog	R&D Systems	AF2729, RRID: AB_2150103
Nestin	Milipore	MAB5326, RRID: AB_2251134
Sox2	Santa Cruz	sc-17320, RRID: AB_2286684
FoxA2	Santa Cruz	sc-101060, RRID: AB_1124660
Tuj1	Biolegend	801202, RRID: AB_10063408
TH	Abcam	Ab112, RRID: AB_297840
Girk2	Abcam	Ab65096, RRID: AB_1139732
Nurr1	Santa Cruz	sc-990, RRID: AB_2298676
activated caspase 3	Cell Signaling	9661, RRID: AB_2341188
anti mouse 488	Life Technology	A21202, RRID: AB_141607
anti rabbit 488	Life Technology	A21206, RRID: AB_141708
anti goat 488	Life Technology	A11055, RRID: AB_2534102
anti mouse 567	Life Technology	A11036, RRID: AB_143011
anti rabbit 567	Life Technology	A10040, RRID: AB_2534016
anti goat 567	Life Technology	A11056, RRID: AB_142628
anti mouse 647	Life Technology	A311571
NFκB /p65	Santa Cruz	sc-8008, RRID: 628017
NFκB /p50	Abcam	Ab32360, RRID: AB_776748
Act1	Santa Cruz	sc-100647, RRID: AB_2209557
β-actin	Sigma-Aldrich	A1978, RRID: AB_476692
TATA	Abcam	Ab51841, RRID: AB_945758
IL-17R	Abcam	Ab5112-1, RRID: AB_10897797
MHC class I	Santa Cruz	sc-55582, RRID: AB_831547
Biological Samples		
Human substantia nigra tissue (non-demented control, F, 71 years, Braak 0)	Netherlands Brain Bank (NBB) (paraffin embedded)	1992-027
Human substantia nigra tissue (non-demented control, M, 72 years, Braak 0)	NBB (paraffin embedded)	1993-05

(*Continued on next page*)

Continued

REAGENT or RESOURCE	SOURCE	IDENTIFIER
Human substantia nigra tissue (Parkinson's disease, M, 71 years, Braak 3)	NBB (paraffin embedded)	2010-113
Human substantia nigra tissue (Parkinson's disease, F, 71 years, Braak 2)	NBB (paraffin embedded)	2012-041
Human substantia nigra tissue (Parkinson's disease, M, 77 years, Braak 3)	NBB (paraffin embedded)	2013-061
Chemicals, Peptides, and Recombinant Proteins		
CHIR99021	Tocris	4423
Cycloheximide (CHX)	Sigma Aldrich	C104450
Glial Derived Growth Factor (GDNF)	Peprotech	450-10
Purmorphoamine (PMA)	Tocris	4551
Fibroblast Growth Factor 8 (FGF8)	Peprotech	100-25
LDN	Tocris	6053
SB 431542	Tocris	1614
Rho Kinase Inhibitor (RI) Y27632	Tocris	1254
Adenosine 3,5-cyclic monophosphate (cAMP)	Applichem	A0455
Transforming Growth Factor (TGF)β	Peprotech	AF-100-36E
Recombinant human IL-17/IL-17A	R&D Systems	7955-IL-025/CF
Recombinant human TNFa	R&D Systems	210-TA-005
Recombinant human IL-1b	R&D Systems	201-LB
IL-17 neutralizing antibody	Sino Biological	12047-M237-200
Secukinumab	Novartis	Cosentyx
IL-17R neutralizing antibody	Sino Biological	10895-R004-500
GE Healthcare ECL Select	Fisher Scientific	12393969
DAPI	Thermo Fisher	D1306
CD3 CD28 Dynabeads	Thermo Fisher	11131D
OpTmizer T Cell Expansion SFM Medium	Thermo Fisher	A1048501
Accutase	Sigma-Aldrich	10828010
Geltrex	GIBCO	A1569601
KO serum replacement	Thermo Fisher	10828010
KO_DMEM	Thermo Fisher	10829018
Non-essential amino acids	Thermo Fisher	11140068
β-Mercaptoethanol	Sigma-Aldrich	M6250
Monensin	Sigma-Aldrich	M5273
Ionomycin	Calbiochem	407952
Phrobol Myristate Acetate	Sigma-Aldrich	P8139
Lymphoflot	BioRad	824012
CD3 microbeads	Miltenyi	130-050-101
Saponin	Sigma-Aldrich	47036
N2	Thermo Fisher	A1370701
B27	Thermo Fisher	12587001
Neurobasal	Thermo Fisher	21103049
DMEM/F12	Thermo Fisher	11320033
Astrocyte Medium	ScienCell Research Laboratories	1801
NeuroFluor NeuO	Stem Cell Technologies	01801
Collagenase IV	Thermo Fisher	17104019
mTeSR	Stem Cell Technologies	85850

(*Continued on next page*)

Continued

REAGENT or RESOURCE	SOURCE	IDENTIFIER
Critical Commercial Assays		
TUNEL assay	Life Technologies	C10245
SYBR Green PCR Master Mix	Applied Biosystems	4309155
QuantiTect Reverse Transcription Kit	QIAGEN	205311
IL-17 Cytoscreen kit, BIOSOURCE for IL-17	Thermo Fisher	AC1591
BCA Assay	Thermo Fisher	23227
Deposited Data		
RNA-Seq data (FastQ files)	dbGAP	accession nnumber pending; contact authors for raw data
Experimental Models: Cell Lines		
Human primary cerebellar astrocytes	ScienCell Research Laboratories	1810
Oligonucleotides		
Primers for RT-qPCR, see Table S3	This paper	N/A
Software and Algorithms		
ImageJ version 5.2.1	NIH	RRID: SCR_003070
GraphPad Software Prism 6	GraphPad Software Inc.	RRID: SCR_002798
FlowJo software 8.5.3	FlowJo, LLC	RRID: SCR_008520
CytExpert software	Beckman Coulter	RRID: N/A

CONTACT FOR REAGENT AND RESOURCE SHARING

Further information and requests for resources and reagents should be directed and will be fulfilled by the Lead Contact, Iryna Prots (iryna.prots@uk-erlangen.de).

EXPERIMENTAL MODEL AND SUBJECT DETAILS

Subjects

Postmortem brain tissues were obtained from the Netherlands Brain Bank (NBB) from 3 early-stage sporadic PD patients and 2 age- and sex-matched controls (NBB #1043, Table S2 and Key resources table). Peripheral venous blood samples were collected from 10 patients from the movement disorder clinic of the Department of Molecular Neurology (Universitaetsklinikum Erlangen, Erlangen, Germany) with idiopathic PD and 10 age- and sex-matched controls (Figure S1A). HiPSC were generated from 3 sporadic PD patients and 3 sex- and age-matched controls (Table S2). Sample size of patient and control groups for postmortem brain tissue and peripheral blood analyses, and for hiPSC generation was taken as an optimal size requiring reasonable performing time and allowing statistic evaluation of the results. Control individuals were defined as those if they did not have any neurological disease. Controls and patients with a history of cancer, infectious or autoimmune diseases, or anti-inflammatory treatment within the past three months prior to the study inclusion were excluded. Patients were included into PD group based on the PD diagnosis. PD was diagnosed by board examined movement disorder specialists according to consensus criteria of the German Society of Neurology, which are similar to the UK PD Society Brain Bank criteria for diagnosis of PD. PD patients were defined as having a sporadic disease by the absence of known PD-causing genetic mutations (PARK 1-18). Study approval was granted by the local ethics committee (No. 4120 and No. 4485, Universitaetsklinikum Erlangen, FAU Erlangen-Nuernberg, Erlangen, Germany) and all participants gave written informed consent prior to inclusion into the study. All PD patients were at early stages of PD (H&Y: 1-2 and Braak stage 2-3) and were under dopaminergic substitution therapy (Figure S1A and Table S2). Since PD is predominantly affecting male population, we designed our study cohorts accordingly consisting of 70%–90% of male and 10%–30% of female samples/subjects. Furthermore, we do not expect a strong impact of sex on the immunological parameters tested in this study, while the sample size of our cohorts would be too small in order to statistically prove a possible influence.

METHOD DETAILS

Human T lymphocyte isolation

Venous blood was withdrawn between 8 and 10 am and collected in heparin-containing syringes. To isolate PBMCs, 20 mL blood was diluted with 20 mL Phosphate-buffered saline (PBS) and centrifuged over a layer of 10 mL ficoll at 600 g for 30 minutes (min) at room temperature (RT). Subsequently, PBMCs were labeled with magnetic beads to isolate CD3+ T lymphocytes according to the manufacturer's instructions. The purity of isolated T lymphocytes was assessed by flow cytometry using staining for CD3 and was

normally > 95%. More than 98% of the cells were viable after purification. CD3+ T cells were counted and used for surface staining, *ex vivo* stimulation, or activation prior to co-culture with human neurons. *Ex vivo* stimulation for screening of surface markers and Th-specific cytokines was performed in CTS OpTmizer T Cell Expansion SFM medium supplemented with 2 μM Monensin, 1 μM Ionomycin and 20 ng/ml Phrobol Myristate Acetate for 5 hours (hr) at 37°C. Subsequently, cells were harvested, fixed with 4% paraformaldehyde (PFA) for 10 min at 37°C and permeabilized with 0.1% Saponin prior to surface and intracellular staining.

Flow cytometry analysis

For flow cytometry analysis, T lymphocytes or hiPSC were washed with 1 mL FACS-PBS (PBS, 2% FCS, 0.01% NaN3). For surface staining, 0.1×10^6 cells/staining were incubated with saturating amounts of fluorescently labeled antibodies for 15 min at 4°C in the dark. For intracellular staining, 0.5×10^6 cells/staining were incubated with saturating amounts of fluorescently labeled anti-cytokine antibodies for 30 min at 4°C in the dark. All primary antibodies used are listed in the Key resources table. Cells were washed and collected in 300 μl FACS-PBS. Flow cytometry was performed using FACS Calibur flow cytometer (BD Biosciences) or Cytoflex (Beckman Coulter, Inc.) and analyzed using FlowJo software 8.5.3 (FlowJo, LLC) or CytExpert software (Beckman Coulter, Inc.). Fluorescence signals were determined using an appropriate electronic compensation to exclude emission spectra overlap.

Generation and cultivation of MBN

HiPSC were reprogrammed using retroviral transduction of the transcriptions factors OCT3/4, c-MYC, SOX2 and KLF4 as previously described (Havlicek et al., 2014). The Institutional Review Board approval (Nr. 4120: Generierung von humanen neuronalen Modellen bei neurodegenerativen Erkrankungen) and informed consent forms are on file at the movement disorder clinic at the Department of Molecular Neurology, Universitaetsklinikum Erlangen (Erlangen, Germany). All the hiPSC lines were screened for pluripotency and for stable karyotype using the G-banding chromosomal analysis (data not shown). Two hiPSC clones per individual of the 3 PD patients and 3 age- and sex-matched controls (Table S2) were differentiated into MBN as previously described [16]. In brief, hiPSC were detached five to seven days after passaging using collagenase IV (GIBCO® Thermo Fisher Scientific) treatment for 20 min at 37°C, 5% CO2. Cell colonies were resuspended in human embryonic stem cells (hESC) medium (80% KO-DMEM, 20% KO serum replacement, 1% non-essential amino acids, 1% Penicillin/Streptavidin, 1mM β-Mercaptoethanol supplemented with the small molecules 1 μM LDN, 10 μM SB, 3 μM Chir, and 0.5 μM Purmorphoamine [PMA]) and cultured on ultra-low adhesion plates. After 2 days of incubation, the medium was changed to N2B27 medium (50% DMEM/F12, 50% Neurobasal Medium, 1:200 N2, 1:100 B27 supplemented with the same small molecules). On day four, the medium was changed to smNPC medium (N2B27 medium supplemented with 3 μM Chir, 0.5 μM PMA and 150 μM Ascorbic acid [AA]). After 2 more days of suspension culture, cell colonies were replaced on geltrex-coated 12-well plates in smNPC medium supplemented with Rho kinase inhibitor Y27532 (RI). Medium was changed every other day and cells were passaged once a week as single cells at ratios of 1:6 to 1:9. After at least five passages, smNPCs were differentiated into MBN. For this aim, two days after passaging, the medium was exchanged to N2B27 medium supplemented with 100 ng/ml FGF8, 1 μM PMA and 200 μM AA. After eight days, medium was changed to maturation medium (N2B27 supplemented with 100 ng/ml FGF8, 10 ng/ml GDNF, 10 ng/ml TGFb, 200 μM AA, and 500 μM Dibutyryl-cAMP [dbcAMP]). On the next day, cells were passaged at ratios of 1:2 – 1:3 as single cells after accutase treatment, plated onto geltrex-coated 4-well chamber slides (Ibidi) or 12-well plates and further cultured for at least 2 weeks in maturation medium with two times media change per week.

Co-culture of MBN with T cells/ cytokines

To analyze the effect of T lymphocytes on MBN, human autologous co-culture experiments were performed. MBN were seeded at a density of 100,000 cells/chamber of a 4-well chamber slide and 150,000 cells/well of a 12-well plate. To initialize the co-culture, medium was changed to a CTS OpTmizer T Cell Expansion SFM medium supplemented with the neurotrophic factors as used for the maturation of the neurons (described before). Isolated T lymphocytes were activated using CD3 CD28 dynabeads according to the manufacturer's instructions to achieve polyclonal T cell activation by triggering T cell receptor and costimulatory molecules using antibodies against CD3 and CD28, respectively. Activated T lymphocytes were added to MBN from the same individual at a ratio of 1:1 (or 0.1:1, 10:1) and cultured for 3 days (or 1 - 10d) at 37°C, 5% CO2. After 3 days of neuron:T lymphocyte co-culture, the supernatants were collected for enzyme-linked immunosorbent assay (ELISA), whereas neurons were either collected for gene or protein expression analyses (12-well plates) or further processed for cell death and neurite outgrowth analyses (4-well chamber slides). Three-day co-culture time point was chosen for the following reasons: 1) while defining the co-culture conditions, the three-day cultivation time point of either T lymphocytes or control neurons in a Serum-Free Lymphocyte Medium led to the optimal activation of T lymphocytes and lowest neuronal cell death (Figure S3A, Medium #7); 2) a previous study (Giuliani et al., 2003) investigated cell death of primary neurons after co-culture with T lymphocytes and found that the manifestation of T lymphocyte-mediated neurotoxicity is evident after 3 days of culture. To exclude potential effect of CD3 CD28 dynabeads on neurons, we cultured them with neurons in the absence of T lymphocytes, but did not detect any effect.

As an alternative to co-cultures with T lymphocytes, MBN were treated with different doses of recombinant IL-17A (0.15 ng/ml, 0.5 ng/ml), IL-1b (0.03 ng/ml, 0.3 ng/ml) or TNFa (10 ng/ml, 100 ng/ml) for 3 days, according to the amount of cytokine found in the supernatant (low concentration) or 10-times higher (high concentration). Rescue experiments were performed by adding 0.62 μg/ml anti-IL-17A neutralizing antibodies (either from Sino biological Inc., or secukinumab) or 1.06 μg/ml anti-IL-17R neutralizing antibodies to neuronal cultures prior to adding T lymphocytes.

Culture of human astrocytes

Human cerebellar astrocytes were cultured according to the manufacturer's instructions. Briefly, 5000 astrocytes/cm^2 were cultured in astrocyte medium with supplements (ScienCell Research Laboratories) in uncoated T75 flasks or 6-well plates at 37°C, 5% CO_2. Full media changes were performed every three days, and astrocytes were passaged after reaching approximately 90% confluency using trypsin/EDTA treatment for 3 min at RT. For the cytokine experiments, astrocytes were treated with IL-17 (0.15 ng/ml and 0.5 ng/ml) for 3 days.

Immunofluorescence and image analysis

Cells, including hiPSC, smNPC and differentiated MBN, were fixed with 4% PFA at RT for 10 min. Fixed cells were blocked for 1 hr with PBS containing 3% donkey serum and 0.1% Triton X-100 before adding the primary antibodies (Key resources table) for an incubation overnight at 4°C. For the MHC class I staining, fixed neurons were blocked with PBS containing 5% donkey serum without Triton X-100 in order to determine only surface MHC class I. Subsequently, cells were incubated with the appropriate fluorescently labeled secondary antibodies (Key resources table) for 1 hr at RT, followed by 2 min incubation with DAPI (10 μg/ml) at RT to stain the nuclei. Finally, stained cells were mounted on an object glass using 10 μl of mounting solution (Aqua-Poly/Mount, Polysciences). After drying overnight at RT in the dark, the object glasses were stored at 4°C in the dark. Images were taken at the Axio Observer.Z1 fluorescence microscope with ApoTome technology or LSM 780 confocal laser scanning microscope (both from Carl Zeiss). Images were quantified using the cell counter plugin and the ImageJ software (version 5.2.1).

Cell death analysis

To determine the cell death rate of neurons, TUNEL assay was applied according to the manufacturer's instructions. In parallel, cells from the same experiment were pretreated with ice-cold acetic acid and ethanol (2:1) for 5 min at -20°C and stained with antibody against aCASP3. TUNEL and aCASP3 are characteristic for different stages of cell death: TUNEL labels fragmented DNA, which occurs at a late cell death stage, whereas aCASP3 is an early event during apoptosis. The numbers of double-positive cells (TUBB3/TUNEL, TUBB3/aCASP3, or TH+/TUNEL, TH-/TUNEL) were calculated using ImageJ software to determine the apoptosis rate of total neurons (TUBB3+) or midbrain dopaminergic (TH+) or TH- neurons. At least 500 cells were analyzed for each individual from two independent hiPSC clones. The neurite length was determined in TH+ neurons in all conditions using the simple neurite tracer plugin (ImageJ, version 5.2.1).

Cytokine analysis

IL-17 in the supernatants of the co-cultures was analyzed by ELISA according to the manufacturer's instructions. In brief, cell culture supernatants were equilibrated to room temperature and 100 μl of the supernatant were mixed with 50 μl of Solution A and 50 μl of Biotin conjugate per well of the according ELISA plate and incubated on a shaking plate at 700 rpm. After 2 hr of incubation, the plate was washed three times using the Biosource Wash Solutions. Afterward, 100 μl of diluted Streptavidin-Horseradish peroxidase (HRP) conjugate was added to each sample and incubated for 30 min at RT on a shaking plate at 700 rpm. Following three washing steps, 100 μl of Chromogenic solution was added to each well and incubated for 15 min. Consequently, the reaction was stopped by adding 100 μl Stop solution before measuring the absorbance at 450 nm using SpectraMax 190 Microplate Reader (Molecular Devices). All measured values were normalized to standard samples provided in the ELISA kit.

Gene expression analysis

For total RNA isolation, cells were lysed using QIAzol phase separation buffer followed by column separation using the RNeasy kit according to the manufacturer's instructions. Five hundred ng of total RNA was reversely transcribed into cDNA in 20 μl reaction solution using the QuantiTect Reverse Transcription Kit according to the manufacturer's instructions, including a DNase treatment step. One μl of cDNA was used for a qRT-PCR reaction. qRT-PCR was performed as previously described (Sommer et al., 2016). Forward and reverse primer pairs (Sigma-Aldrich) for SYBR Green PCR are listed in Table S3.

Library preparation and RNA sequencing

Libraries for next-generation sequencing were prepared with total RNA isolated from untreated and IL-17-treated cells with the TruSeq® RNA Sample Preparation Kit v2 (Illumina) according to the manufacturer's instructions. Finally, quality control with a Bioanalyzer® (Agilent) and sequencing with a HiSeq 1000 sequencer (Illumina) were performed. For this purpose, all libraries were quantified using the KAPA SYBR FAST ABI Prism Library Quantification Kit (Kapa Biosystems). Equimolar amounts of each library were used for cluster generation on the cBot with the TruSeq SR Cluster Kit v3 (Illumina). The sequencing run was performed on a HiSeq 1000 instrument (Illumina) using the indexed, 50 cycles single read (SR) protocol and the TruSeq SBS v3 Kit (Illumina). Image analysis and base calling resulted in .bcl files that were then converted into .fastQ files by the CASAVA1.8.2 software.

RNA-Seq analysis

FastQ files were aligned to the human genome (hg19) using STAR under previously published conditions (Kapeli et al., 2016). Aligned sam-files were annotated with gencode.v19 and features counted using SubReads featureCounts. DESeq2 was used to determine differential expression (Kapeli et al., 2016). Stringent criteria were set to determine significantly dysregulated genes: adjusted p value below 0.05 and log2FC of greater than one. To lessen false positives due to high variability of lowly expressed transcripts, only genes

with a mean expression value of greater than one RPKM throughout the dataset were considered. Control and PD samples were analyzed as two independent datasets. Hierarchical clustering and heatmaps representing z-scores were generated using the seaborn package in python.

To determine if the promoters of dysregulated genes were enriched in certain TFBS, locations of IL-17-associated transcription factors CEBPB, NFκB, cFos and cJun were extracted from UCSC's database of 161 ChIP-seq experiments from ENCODE (Data version: ENCODE Mar 2012 Freeze) (Consortium and ENCODE Project Consortium, 2012). Promoters were defined as 2.5kb upstream of the transcription start site. The intersections in TFBS in promoters were determined with bedtools and significance of enrichment was calculated using the hypergeometric test in R, followed by Benjamini-Hochberg correction. Significant enrichment was considered if the adjusted p value was below 0.05.

Western blot analysis

For the protein analysis, neurons were harvested and washed twice with cold PBS, gently resuspended in cold hypotonic buffer (20 mM Tris pH 7.4, 10 mM NaCl, 3 mM $MgCl_2$ supplemented with protease and phosphatase inhibitors) and incubated for 15 min at 4°C. After adding 10% NP40, homogenates were centrifuged for 15 min at 3000 rpm at 4°C to separate supernatant 1 (S1; cytosolic fraction) from pellet 1 (P1; nuclear pellet). While S1 was collected, P1 was resuspended in cold cell extraction buffer (100 mM Tris pH 7.4, 2 mM Na_3VO_4, 100 mM NaCl, 1% Triton X-100, 10% glycerol, 1 mM EDTA, 1mM EGTA, 0.1% SDS, 1 mM NaF, 0.5% deoxycholate, 20 mM $Na_4P_2O_7$ supplemented with protease and phosphatase inhibitors) and incubated for 30 min at 4°C, and then posteriorly centrifuged for 30 min at 14000 rpm, 4°C. The resulting supernatant (S2; nuclear fraction) was collected. The protein concentrations of lysed samples were determined using the bicinchoninic acid assay (Pierce BCA Protein Assay Kit). Equal amounts of total protein (20 μg) were separated on 10% SDS-PAGE and transferred onto PVDF membranes (Bio-Rad). Blots were probed using primary antibodies (Key resources table) and HRP-conjugated secondary antibodies (Key resources table). For visualization of signals, the GE Healthcare ECL Select and the Fujifilm LAS 3000 device were used. The signal intensities of the respective proteins were normalized to that of β-actin (cytoplasmic fractions) or TATA (nuclear fractions).

Patch clamp experiments

Whole-cell patch clamp recordings were performed at RT using an EPC 10 amplifier (HEKA electronics) in artificial cerebrospinal fluid bubbled with 95% O_2 and 5% CO_2 (125 mM NaCl, 3 mM KCl, 1 mM $CaCl_2$, 1 mM $MgCl_2$, 1.25 mM NaH_2PO_4, 25 mM $NaHCO_3$ and 10 mM d-glucose; pH 7.4). The pipette solution contained 4 mM NaCl, 135 mM K-gluconate, 3 mM $MgCl_2$, 5 mM EGTA, 5 mM HEPES, 2 mM Na_2-ATP and 0.3 mM Na_3-GTP (pH 7.25). Neuronal cells were identified by NeuroFluor NeuO (Stemcell) staining according to manufacturer protocol.

QUANTIFICATION AND STATISTICAL ANALYSIS

Statistical details of experiments

Each experiment was performed with 12 neuronal lines, where each line was differentiated from two hiPSC clones for each individual for co-culture, immunofluorescence staining, and gene and protein expression, with their respective biological/technical numbers (n) indicated in the figure legends. The flow cytometry analysis of resting or *ex vivo* stimulated T lymphocytes was performed with blood from 10 PD patients and 10 sex- and age-matched controls. For flow cytometry analyses, at least 20,000 events were collected. The postmortem analysis was performed with 3 SN samples from sporadic PD patients and 2 age- and sex-matched controls. Differences between the two groups were analyzed with two-tailed unpaired Student's t test. When more than two groups were compared, differences were analyzed with one- or two-way-ANOVA followed by Sidak or Tukey multiple comparisons tests as indicated. In all analyses, p values of less than 0.05 were considered significant. All statistical tests were conducted with GraphPad Prism 6 Software (GraphPad Software, Inc.).

DATA AND SOFTWARE AVAILABILITY

The RNA-seq data will be deposited in the database of Genotypes and Phenotypes (dbGaP) and the accession number is currently pending. In the interim, please send requests for human RNA-seq data related to this manuscript directly to the authors, and we will supply the relevant raw data.

Cell Stem Cell, Volume *23*

Supplemental Information

Th17 Lymphocytes Induce Neuronal Cell Death in a Human iPSC-Based Model of Parkinson's Disease

Annika Sommer, Franz Maxreiter, Florian Krach, Tanja Fadler, Janina Grosch, Michele Maroni, Daniela Graef, Esther Eberhardt, Markus J. Riemenschneider, Gene W. Yeo, Zacharias Kohl, Wei Xiang, Fred H. Gage, Jürgen Winkler, Iryna Prots, and Beate Winner

	T cell subpopulation	PD (n=10) [%]	Control (n=10) [%]	p-value
Resting	CD3+ CD4+	70.67 ± 11.85	75.96 ± 7.57	0.113
	CD3+ CD8+	19.31 ± 12.50	19.99 ± 8.07	0.924
	CD4+ CD25+	6.88 ± 1.95	17.06 ± 9.32	***0.028***
	CD3+ CD127lo	7.37 ± 2.67	8.44 ± 2.28	0.231
	CD3+ CD4+ CD54+	13.98 ± 4.89	7.91 ± 5.30	0.131
	CD3+ CD4+ CD95+	49.95 ± 12.58	40.32 ± 20.14	0.216
	CD3+ CD4+ CD178+	1.61 ± 1.24	0.97 ± 0.67	0.173
	CD3+ CD8+ CD54+	37.36 ± 21.12	38.61 ± 34.40	0.923
	CD3+ CD8+ CD95+	43.22 ± 24.74	41.05 ± 23.76	0.844
	CD3+ CD8+ CD178+	2.61 ± 3.31	0.98 ± 0.95	0.152
	DR1+ CD3+ CD4+	79.11 ± 21.85	99.16 ± 1.27	0.182
	DR1+ CD3+ CD8+	80.80 ± 15.99	97.76 ± 1.95	0.134
	DR2+ CD3+ CD4+	4.62 ± 3.27	17.90 ± 12.11	***0.035***
	DR2+ CD3+ CD8+	2.56 ± 3.94	10.68 ± 5.65	***0.011***
	DR3+ CD3+ CD4+	6.92 ± 2.61	5.51 ± 1.36	0.430
	DR3+ CD3+ CD8+	8.90 ± 3.98	14.13 ± 5.86	0.177
	DR5+ CD3+ CD4+	25.47 ± 32.08	35.98 ± 35.40	0.551
	DR5+ CD3+ CD8+	31.19 ± 33.03	35.98 ± 32.74	0.782
Stimulated	CD4+ CD25+	10.36 ± 5.27	7.72 ± 3.08	0.188
	CD3+ CD127lo	5.30 ± 1.73	6.69 ± 1.79	0.055
	CD3+ CD4+ CD54+	11.96 ± 6.86	13.43 ± 8.14	0.668
	CD3+ CD4+ CD95+	36.81 ± 15.23	34.32 ± 11.09	0.681
	CD3+ CD4+ CD178+	4.05 ± 2.94	1.7 ± 0.80	***0.026***
	CD3+ CD8+ CD54+	39.44 ± 28.21	35.81 ± 17.02	0.732
	CD3+ CD8+ CD95+	42.23 ± 25.76	41.98 ± 19.53	0.981
	CD3+ CD8+ CD178+	13.65 ± 8.86	4.23 ± 2.46	***0.005***
	DR1+ CD3+ CD4+	2.78 ± 1.17	6.92 ± 3.45	0.075
	DR1+ CD3+ CD8+	82.53 ± 10.05	74.75 ± 16.62	0.497
	DR2+ CD3+ CD4+	11.25 ± 10.19	22.26 ± 17.05	0.133
	DR2+ CD3+ CD8+	21.60 ± 13.46	24.36 ± 17.89	0.727
	DR3+ CD3+ CD4+	3.35 ± 1.01	2.26 ± 0.23	0.224
	DR3+ CD3+ CD8+	17.07 ± 8.49	8.47 ± 10.08	0.328
	DR5+ CD3+ CD4+	11.27 ± 11.69	14.99 ± 11.05	0.581
	DR5+ CD3+ CD8+	20.91 ± 5.35	17.54 ± 12.85	0.518
	IFNg+	14.77 ± 8.35	10.27 ± 6.41	0.193
	IL-2+	9.20 ± 9.41	4.72 ± 5.28	0.205
	IL-4+	1.64 ± 1.70	1.45 ± 0.83	0.755
	IL-10+	1.09 ± 0.69	2.09 ± 1.48	0.070
	IL-17+	1.67 ± 0.75	0.75 ± 0.35	***0.002***

Table S1 (related to Fig. 1): Flow cytometry analysis of resting and stimulated T lymphocytes. T lymphocytes from PD patients and controls were characterized by flow cytometry for T cell surface

markers and dopamine receptors (DR1-5) either directly after isolation (resting) or after 5 hours of *ex vivo* stimulation (stimulated). After stimulation, cells were additionally stained intracellularly for cytokine production (IFNg, IL-2, IL-4, IL-10, IL-17). Experiments were performed with 10 PD patients and 10 controls (n = 10 per group). Data are shown as means ± SD. p-values are marked in bold and italic when they reach a significance threshold of 0.05 by two-tailed Student´s t-test. CD = cluster of differentiation, IL = interleukin.

PD patient and control postmortem brain samples					
Sample ID	**Barcode**	**Gender**	**Age at death**	**PMD (hr)**	**Braak stage**
PD-SN-1	2010-113	M	71	5:05	3
PD-SN-2	2012-041	F	71	9:05	2
PD-SN-3	2013-061	M	77	3:10	3
C-SN-1	1992-027	F	71	9:00	0
C-SN-2	1993-05	M	77	4:30	0

PD patient and control cohorts used for the co-culture experiments							
Cell Line	**Abbre-viation**	**Group**	**Age at donation**	**Gender**	**H&Y**	**LEDD**	**Color code**
UKERiAY6-R1-3	PD1-1	PD	37	M	2	1050	
UKERiAY6-R1-4	PD1-2						
UKERiPX7-R1-1	PD2-1	PD	49	M	1	850	
UKERiPX7-R1-2	PD2-2						
UKERi88H-R1-1	PD3-1	PD	63	F	1	400	
UKERi88H-R1-2	PD3-2						
UKERi33Q-R1-2	C1-1	Control	45	F	-	-	
UKERi33Q-R1-6	C1-2						
UKERiO3H-R1-1	C2-1	Control	71	M	-	-	
UKERiO3H-R1-5	C2-2						
UKERi82A-R1-1	C3-1	Control	66	F	-	-	
UKERi82A-R1-2	C3-2						

Table S2 (related to Fig. 1 and Fig. 2): PD patient and control postmortem brain samples and cohorts used for the co-culture experiments. Postmortem brain tissues were obtained from the Netherlands Brain Bank from 3 early-stage sporadic PD patients (Braak stage 2-3; PD-SN-1-3) and 2 age- and sex-matched controls (C-SN-1-2). Human induced pluripotent stem cells (hiPSC) generated from fibroblasts of 3 PD patients (PD1-3) and 3 age- and sex-matched controls (C1-3) were used for all co-culture experiments. The color code is used to label individual patients or controls in Fig. 1h and Fig. S1c. PD = Parkinson´s disease, ID = identification, C = Control, SN = substantia nigra, PMD = postmortem delay, hr = hours, M = male, F = female, H&Y = Hoehn and Yahr, LEDD = Levodopa equivalent daily dose in mg.

Gene	Forward (5´-3´)	Reverse (5´-3´)
IL17R	ACT GAG GCA TCA CCA CAG G	TCT TGG ACT GGT GGT TTG G
IL1R	TGT GGA AAA TCC TGC AAA CA	GGA ATC CCT GTA CCA AAG CA
TNFaR	TGC CAT GCA GGT TTC TTT C	TCT GGG GTA GGC ACA ACT TC
STK36	GAA CAT CCT CCT CGC CAA G	GGT GTG CCT TTG ATG GAT G
SLC9A3	CCA TGT CAA CGA GGT CCT G	CGC CAC GAA AGA TTC AAA C
ABCA7	TCT ACC AGG GCC ACA TCA C	ATG AAG GCA GAG CCA CCA C
PCSK4	CGG GCA GTA CTT TCA CCT G	CAC GAC AGA GCG TTT CAC C
HPRT	CCT GGC GTC GTG ATT AGT G	TCC CAT CTC CTT CAT CAC ATC
β-actin	TTT TTG GCT TGA CTC AGG ATT T	GCA AGG GAC TTC CTG TAA CAA C
2bm	GAG GCT ATC CAG CGT ACT CC	AAT GTC GGA TGG ATG AAA CC

Table S3 (related to STAR Methods): Primers used for quantitative reverse transcription (qRT)-PCR.

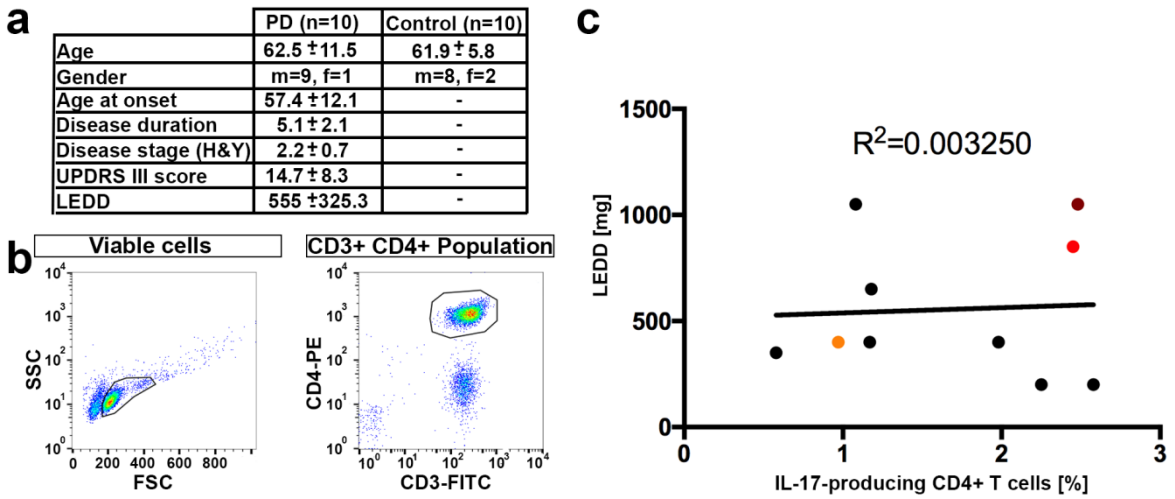

Figure S1 (related to Fig. 1): *Ex vivo* blood study design and correlation analysis of IL-17-producing T lymphocyte frequencies in peripheral blood of PD patients with Levodopa equivalent daily dose (LEDD). T lymphocytes were isolated from peripheral blood of 10 PD patients at an early disease stage and from 10 age- and sex-matched controls (a). m = male, f = female, H&Y = Hoehn and Yahr stage, UPDRS = Unified Parkinson Disease Rating Scale, LEDD = Levodopa equivalent daily dose. Data are shown as mean ± SD. Using a flow cytometry gating strategy, dead cells were excluded and the CD3+ CD4+ T cell population was analyzed (b). SSC = side scatter, FSC = forward scatter, CD = cluster of differentiation. The frequencies of IL-17-producing CD4+ T lymphocytes in the peripheral blood samples of PD patients did not correlate with the dose of LEDD treatment (R^2=0.003250) (c). LEDD represents the amount of dopaminergic treatment per day for each patient. Experiments were performed with 10 PD patients. The colored dots represent the PD patients, whose cells were used for reprogramming and co-culture experiments.

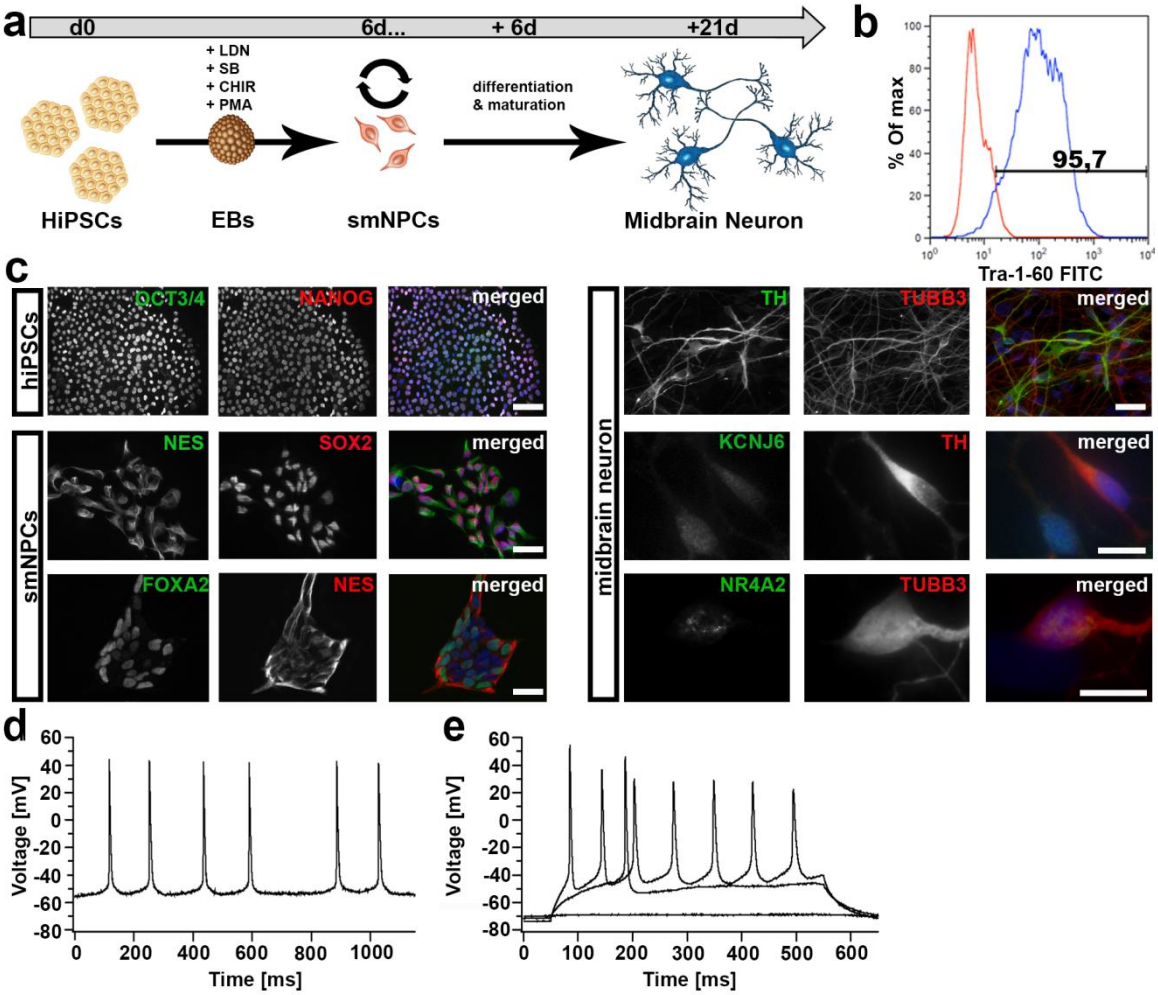

Figure S2 (related to Fig. 2): Generation of midbrain neurons (MBN) by differentiation from human induced pluripotent stem cells (hiPSC) of PD patients and controls. HiPSC derived from PD patients and controls (C) were differentiated into MBN neurons based on previously published protocol (Reinhardt et al., 2013) (a). HiPSC expressed pluripotency markers Tumor recognition antigen (Tra)-1-60 (b), OCT3/4, and NANOG (c), and were differentiated into small molecule neural precursor cells (smNPCs) expressing the characteristic neural precursor markers nestin (NES) and SOX2 as well as the floor plate marker FOXA2 (c). Further differentiation and maturation for 3 weeks resulted in MBN expressing the neuronal marker ß3-tubulin (TUBB3) and dopaminergic markers: tyrosine hydroxylase (TH), Girk2 (KCNJ6), and Nurr1 (NR4A2) (c). Scale bar = 50 µm in (c, left part), 20 µm in (c, right part). Neurons were functionally active, generating spontaneous (d) as well as evoked (e) action potentials. Two hiPSC clones per patient / control were differentiated.

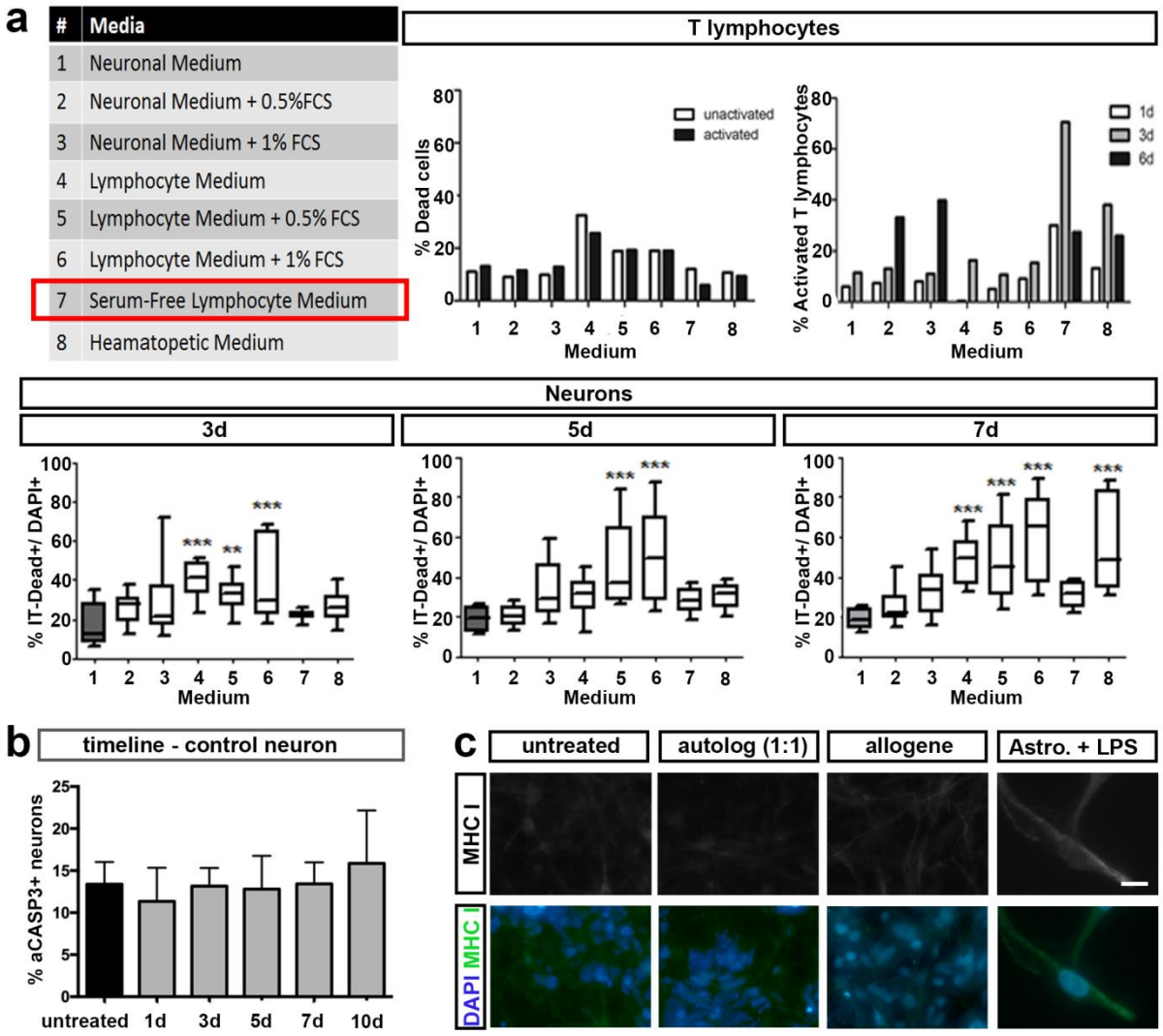

Figure S3 (related to Fig. 2): Optimization of T lymphocyte:neuron co-culture conditions. Eight different media either with or without low concentrations of fetal calf serum (FCS) were tested to determine the medium that supported optimal T lymphocyte *ex vivo* activation and was not toxic to neurons (a). T cells were cultured for 1, 3, or 6 days (d) and neurons for 3, 5 or 7d in the respective media and cell death and/or activation were analyzed. Cell death and activation of T lymphocytes were determined by flow cytometry. Neuronal cell death was determined by the ITdead analysis (a). Control hiPSC-derived neurons were treated with autologous T lymphocytes for 1d up to 10d to exclude any delayed toxic effect (b). Three individual experiments were performed (n = 3 per group). Data are shown as means ± SD. ** - p-value < 0.01, *** - p-value < 0.001 by one-way ANOVA and Sidak test for multiple comparisons. Untreated hiPSC-derived neurons, as well as hiPSC-derived neurons from autologous (autolog 1:1) or allogeneic (allogene) co-cultures with T lymphocytes expressed faint levels of major histocompatibility complex (MHC) class I (green), while astrocytes treated with lipopolysaccharides (LPS, Astro. + LPS) showed expression of MHC class I (c). A representative line of hiPSC-derived neurons from a PD patient is shown.

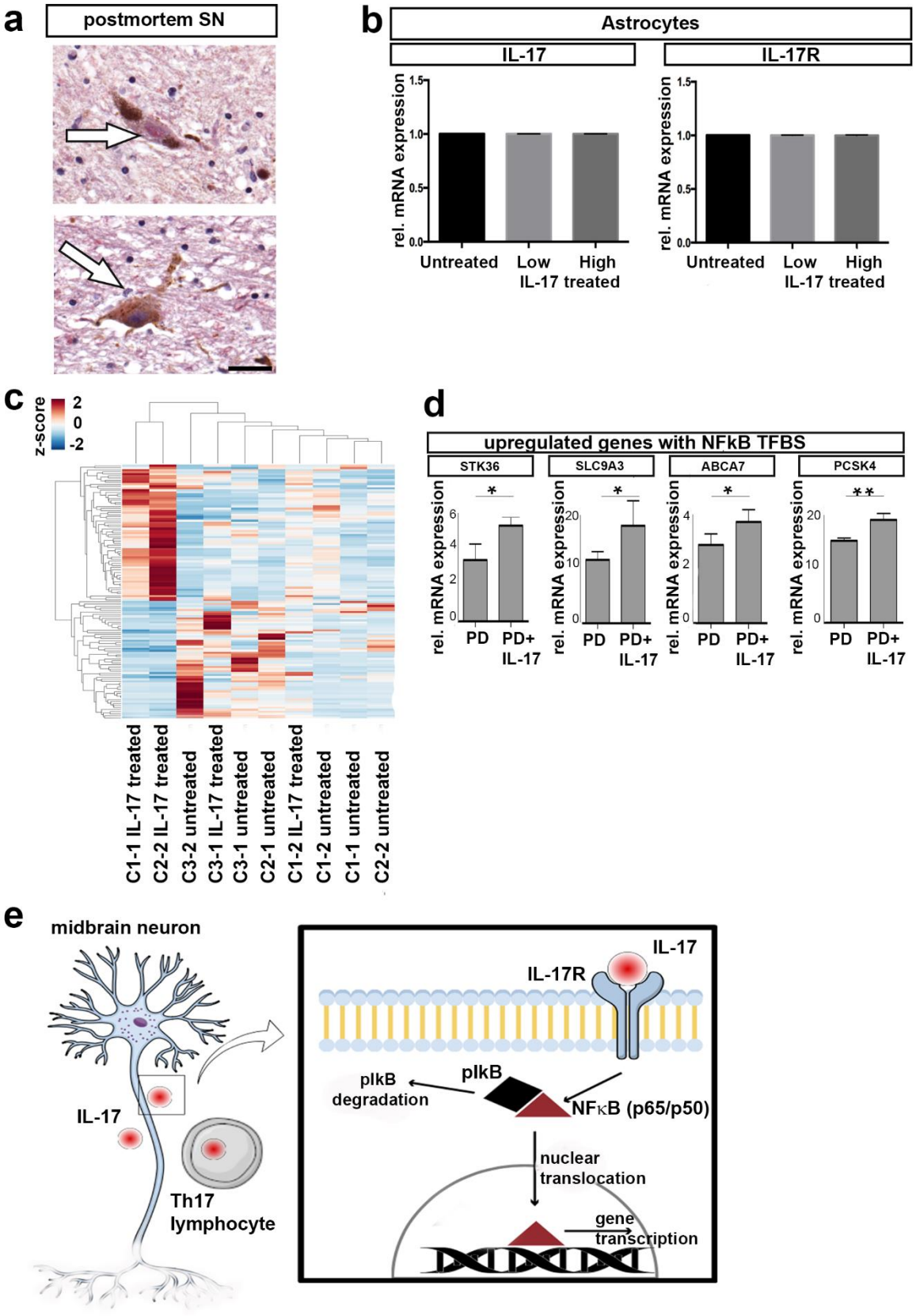

Figure S4 (related to Fig. 3 [a-b] and to Fig. 4 [c-e]): IL-17 receptor (IL-17R) expression in postmortem substantia nigra (SN) neurons of PD patients; and genes, differentially regulated in IL-17-treated PD hiPSC-derived neurons, do not cluster in control samples. Human postmortem

SN samples were stained for IL-17R and positive staining was found in neuromelanin+ neurons in PD SN (as indicated by arrows), but not in controls. Scale bar = 50 µm (a). Human cerebellar astrocytes were treated with low or high concentrations of IL-17 for three days before analyzing the mRNA expression of IL-17 and IL-17R (b). Three individual experiments were performed (n = 3 per group). Data are shown as means ± SD. A heatmap represents 125 genes, differentially regulated in PD hiPSC-derived neuronal samples upon IL-17 treatment, that do not cluster within untreated and IL-17-treated control hiPSC-derived neuronal samples (c). Quantitative reverse transcription (qRT)-PCR analysis confirms elevated expression levels of representative genes (STK36, SLC9A3, ABCA7, PCSK4) upregulated in PD hiPSC-derived neurons after IL-17 treatment with an enrichment of NFκB transcription factor binding sites (TFBS) (d). Experiments were performed with two hiPSC clones for each individual (n=6 per group). Data are shown as means ± SD. *p-value < 0.05, **p-value < 0.01 by Student´s t-test. Model of T cell-released IL-17 and its effect on neurons in sporadic PD, where IL-17 binds to IL-17R, expressed on midbrain neurons, and activates p65/p50 (NFκB) signaling leading to neuronal death (e).